Intranuclear Rodlets:
Dynamic Nuclear Bodies in Pancreatic Beta-Cells;
And, a Novel Variant in Mouse CNS Neurons.

Pavel Milman
PhD Dissertation
Presented to the Department of
Biochemistry, Microbiology and Immunology,
Faculty of Medicine,
University of Ottawa.

Abstract.

Intranuclear rodlets (INRs) are poorly understood intranuclear bodies originally identified within neuronal nuclei on the basis of their unique morphology. Their mechanism of formation, biochemical composition and physiological significance are largely unknown.

To gain insight into the molecular regulators of INR formation, mice with a conditional adult β cell-specific knockout of the master regulator of β-cell metabolism, Lkb1 protein kinase (LABKO mice) were studied. The proportion of beta cells containing INRs was significantly reduced in LABKO mice. Further examination ruled out mTOR and Mark2 as downstream effectors of Lkb1 knockout INR phenotype. Instead it identified the mTOR pathway as an independent regulator of INR formation. To investigate INR changes in a pathophysiological context, β cell INRs were examined in two models of human metabolic syndrome: (1) mice maintained on a high-fat diet and (2) leptin-deficient ob/ob mice. Significant INR reduction was observed in both models. Taken together, our results support the view that INR formation in pancreatic β cells is a dynamic and regulated process. The substantial depletion of INRs in LABKO and obese diabetic mice suggests their relationship to β cell function and potential involvement in diabetes pathogenesis. The significance of these findings was further underscored by the demonstration of INRs in human endocrine pancreas, suggesting their potential relevance to the development of metabolic syndrome in humans.

The existence of biochemically distinct subtypes of INRs has been suggested by previous reports of differential immunological staining of INRs in neurochemically distinct neuronal populations. Here, a novel variant of INR has been identified that is immunoreactive for the 40kDa huntingtin associated protein and ubiquitin; and evidence was provided for the existence of additional INR subtypes sharing ubiquitin immunoreactivity as a common feature. Selective

association of these INRs with melanin concentrating hormone and tyrosine hydroxylase immunoreactive neurons of the hypothalamus and the locus coeruleus was described. It was also demonstrated for the first time that biochemically distinct INR subtypes can co-exist within a single nucleus where they engage in non-random spatial interactions. These findings highlight the biochemical diversity and cell type specific expression of these enigmatic intranuclear structures. On the basis of these findings and previous literature a hypothesis is proposed as to the overall functional significance of INRs in the cell nucleus.

Acknowledgement.

I would like to acknowledge my supervisor John Woulfe, my co-supervisor Doug Gray, members of my advisory committee Fraser Scott and Rashmi Kothari for their guidance throughout my PhD studies.
I would also like to acknowledge my family: my wife Nataliya, my children Alexandra and Nicole, my parents Vladimir Davidovich and Antonina Vasilyevna and my sister Eugenia Milman for their love and unwavering support.
I would like to acknowledge all my friends, past and present; as well as, those whom I may have considered as adverse forces in my life, for fulfilling their respective roles in earnest.

Table of Contents.

List of Abbreviations.

AMPK	-	5′ AMP-Activated Protein Kinase
Arc	-	Arcuate Nucleus
C3T	-	Class III β-Tubulin
cAMP	-	Cyclic Adenosine Mono-Phosphate Nucleotide
CB	-	Coiled Body
CBP	-	CREB (cAMP Response Element Binding Protein) Binding Protein
eIF4E	-	Eukaryotic Translation Initiation Factor 4E
Gems	-	Gemini of Coiled Bodies
Hap1	-	Huntingtin Associated Protein 1
Hap40	-	40 kDa Huntingtin Associated Protein
HFD	-	High-Fat Diet
INR	-	Intranuclear Rodlet
LABKO	-	Lkb1 Adult Beta Cell Knock Out
LC	-	Locus Coeruleus
LHA	-	Lateral Hypothalamic Area
Lkb1	-	Liver Kinase B-1
MCH	-	Melanin Concentrating Hormone
MPTP	-	1-Methyl-4-Phenyl-1,2,3,6-Tetrahydropyridine
NPY	-	Neuropeptide-Y
PABPN1-INR	-	PABPN1 immunoreactive INR
PABPN1	-	Poly(A) Binding Protein Nuclear 1
PML	-	Promyelocytic Leukemia Protein

POMC	-	Pro-opiomelanocortin
PP	-	Pancreatic Polypeptide
SDL-INR	-	SDL.3D10 or GR-P20 antibody immunoreactive INR
SN	-	Substantia Nigra
SON	-	Supraoptic Nucleus
SUMO-1	-	Small Ubiquitin-Like Modifier 1
T2D	-	Type 2 Diabetes
TH	-	Tyrosine Hydroxylase
Ub-Fl76-INR	-	Ub-Fl76 antibody immunoreactive INR
Ub-INR	-	Ubiquitin immunoreactive INR

List of Figures.

List of Tables.

General Introduction.

Elucidating structure-function relationships has traditionally represented an important scientific approach to understanding biological phenomena. From the time when a single cell was recognized as the basic unit of life, efforts to understand cellular function focussed on organelle morphology. In many cases, for example membranous organelles like the Golgi apparatus, structure ultimately predicted function with high fidelity. For other cellular organelles, however, even detailed structural analysis has thus far failed to provide insight regarding physiological significance. It is only relatively recently that various distinct bodies within the cell nucleus have been defined and, remarkably, for most of these, their functional significance has been elucidated. One major exception to this is the intranuclear rodlet (INR). First described in the late 19th century (Mann, 1894), INRs are among the earliest nuclear structures described. Despite that, to this day, their biochemical composition, mechanism of formation and functional significance remain largely unknown. Addressing the biological significance of INRs is the focus of this thesis.

Discovery of INRs.

At the light microscopy level, INRs can be defined as prominent, sharply outlined, typically singular, unbranched, rod-shaped nuclear structures. They were first documented in 1894 by Gustav Mann who in studying changes in neurons induced by "work", described the presence of “peculiar deeply stained crescentic bodies” in the nuclei of sympathetic nerve cells from rabbit occipital lobe (Mann, 1894). Similar rod-shaped nuclear structures were subsequently described by a number of early microscopists using classical light microscopy staining techniques (Holmgren, 1899; Prenant, 1897; Roncoroni, 1895). Notably, INRs were also documented by

Santiago Ramon Y Cajal using his revolutionary reduced silver staining technique. In his morphological description of silver stained neurons, he described “batonnets intranucleaire” and coined the term “Rodlets of Roncoroni” (Cajal, 1909).

Ultrastructure.

Following their initial discovery INRs received little attention until the advent of electron microscopy. The seminal study that triggered a sort of renaissance in INR research by providing continuity between INRs observed by early light microscopists and subsequent electron microscopic observations was published by Siegesmund et al. in 1964 (Siegesmund et al., 1964). In this study, the authors conducted a correlative electron and light microscopic analysis of rabbit olfactory, cerebellar and cortical neurons. Using the reduced silver stain of Ramon Y Cajal the authors documented INRs, or rodlets of Roncoroni, in defined neuronal cell types of selected brain areas. Subsequent electron microscopic examination of the neuronal nuclei in the same neuronal cell types revealed rod-shaped “small bundles of fibrils” which, based on the common overall morphology, were proposed as the ultrastructural counterpart to the rodlets of Roncoroni (Siegesmund et al., 1964).

Ultrastructurally, INRs typically appear as compact bundles of electron dense parallel fibrils aligned along the long axis of the rodlet. Several varying estimates of the fibril diameter appear in the literature ranging from 50 to 100A with apparent consensus being 70±10A (Chandler and Willis, 1966; de Estable-Puig and Estable-Puig, 1970; Lafarga and Palacios, 1977; Masurovsky et al., 1970; Popoff and Stewart, 1968; Seite et al., 1971a; Siegesmund et al., 1964). In addition, lattice or crystalline structures formed from morphologically similar fibrils were reported by Chandler and Willis (1966) who described them as flat or slightly curved sheets “consisting essentially of 2 parallel layers of fibrils crossing each other at an angle of 60° or more

to form a lattice" (Chandler and Willis, 1966). His observations were later confirmed by two independent groups of researchers who produced some of the most detailed ultrastructural studies of INRs available to date (Feldman and Peters, 1972; Seite et al., 1971a). The classification offered by Feldman and Peters (1972) distinguished two types of microfibrillar nuclear structures, rods and sheets, with the latter corresponding to the lattice or crystalline structures reported by Chandler (Chandler, 1966; Chandler and Willis, 1966). Seite et al. have noted that in the cat sympathetic ganglia these fibrillar structures could be associated with an outer core of microtubule arrays. Accordingly their classification of fibrillar nuclear inclusions included three types: a) microfilamentous spindle-shaped, b) microfilamentous-microtubular spindle-shaped, and c) crystalloids composed of layers of fibrillar or tubular lattices (Seite et al., 1971a). Given the ultrustructural similarity of the principal structural component, the ~70A microfiber, and the lack of definitive biochemical markers that could discriminate between rod/spindle vs. sheet/crystalline-shaped structures, the aforementioned structures and their light microscopic counterparts will be referred to collectively as INRs.

Relationship with other nuclear bodies.

Several authors have described spatial associations of INRs with other nuclear compartments such as the nuclear envelope, nucleolus and fibrillogranular or coiled bodies (CB), also known to light microscopists as accessory bodies of Cajal (Clattenburg et al., 1972; Feldman and Peters, 1972; Frink et al., 1978; Masurovsky et al., 1970; Seite et al., 1971a; Toper et al., 1980). Of these, evidence for the association of CBs with INRs appears strongest (Feldman and Peters, 1972; Frink et al., 1978; Masurovsky et al., 1970; Seite et al., 1971a; Toper et al., 1980). Of particular interest are the observations by Masurovsky et al. (1970), who examined the developing neurons of chicken sympathetic ganglia and "highly organized" neuronal cultures of

chicken embryonic sympathetic ganglia. The authors noted that during development, CB formation preceded the formation of intranuclear rod-shaped structures by one to two weeks. Furthermore, they show electron micrographs of CBs in close proximity and even in direct contact with INRs. In some instances, there appeared to be continuity, with some of the material bridging INRs and CBs, leading Masurovsky et al. to suggest that INRs may in fact be derived from CBs (Masurovsky et al., 1970).

Contradictory reports can be found in the literature regarding a physical interaction of INRs with chromatin, whereby some researchers note a narrow zone of euchromatin surrounding most INRs (Chandler and Willis, 1966; Clattenburg et al., 1972; Feldman and Peters, 1972). This has been interpreted to suggest that INRs are surrounded by transcriptionally active chromatin. Others have stressed intimate contact or even continuity between INR fibrils and chromatin (de Estable-Puig and Estable-Puig, 1970; Lafarga and Palacios, 1977) or fine fibrillar material bridging chromatin and the INR (Iwanaga et al., 1981; Tobin et al., 1991).

The significance of each of these associations has been challenged at some point by other researchers who have failed to detect such interactions in their respective experimental systems (Chandler, 1966; Chandler and Willis, 1966; Clattenburg et al., 1972; Dahl, 1970; Feldman and Peters, 1972).

Basic biochemistry.

The proteinaceous nature of INRs was initially established through traditional histochemical staining approaches. INRs were reported to stain with a number of the general protein staining procedures employed by classical histologists. In addition a number of staining techniques for the selective detection of specific amino acids have demonstrated the presence of tyrosine, histidine, tryptophan, arginine, lysine and, possibly, cysteine, aspartic and glutamic

acids (Kim et al., 1970). INRs failed to stain with Feulgen green, Azure B and a number of other nucleic acid stains and did not incorporate tritiated thymidine or uridine, suggesting the lack of nucleic acids in these structures (Kim et al., 1970; Lane, 1969; Masurovsky et al., 1970). Various techniques for the detection of neutral or acidic lipids have failed to stain INRs; however, "subdued" INR staining was observed with acetone-Sudan black B, suggesting the possibility of some bound lipid in INRs (Kim et al., 1970).

Evolutionary aspects.

INRs demonstrate a considerable degree of morphological conservation across the animal kingdom. A comprehensive list of species in which INRs have been documented at the electron microscopic level has been compiled in the textbook by Feronze N. Ghadially (Ghadially, 1997). INRs have been found in the nervous tissue of some of the earliest evolutionary branches of the animal kingdom. Following the split between radially and bilaterally symmetrical organisms, INRs have been reported in Platyhelminthes (flat worms, as represented by planaria), and the more evolved Mollusca (molluscs) and Annelida (segmented worms, represented by leech). Further up the evolutionary tree, INRs have been documented in Chordates across the spectrum from primitive jawless hagfish, to more evolved vertebrates including Gnathostamata (jawed fish), amphibians, avian and mammalian species. The latter account for the majority of reported INR sightings. Among these, are a number of rodent species, including mouse and rat, cat and finally primates, including humans. This remarkable degree of evolutionary conservation suggests that INR structures may have originally developed to serve a common basic nuclear function, but may have evolved to play more specialized and possibly diverse roles in higher vertebrates.

INRs: Functional nuclear bodies or pathological aggregates.

Morphologically discernable intranuclear structures can be broadly classified into two major categories: nuclear bodies and nuclear aggregates. The nuclear bodies represent spatial nuclear compartments that concentrate functional proteins or protein complexes dedicated to a particular nuclear function or a set of mechanistically related nuclear functions. Nuclear bodies occur under normal conditions and are dynamic in nature i.e. they can be induced to assemble or disassemble in response to physiological stimuli. Nucleoli, Cajal and PML bodies are just some of the examples. In contrast, aggregates generally are associated with pathological conditions. They typically contain aberrant, damaged and/or misfolded proteins that have lost their normal biological function and/or may have gained an aberrant function. Although aggregates can sometimes be assigned a pathogenic or even protective role, they typically do not perform any defined physiological function. One of the hallmarks of protein aggregates is their insolubility. Once formed, aggregates tend to persist and may serve as nucleators for the formation of new aggregates. A substantial number of reports of INRs in pathological conditions, either induced by experimental manipulations in laboratory animals (Andrews and Sekhon, 1969; Dixon, 1970; Gambetti and Gonatas, 1967; Pinching and Powell, 1971; Popoff and Stewart, 1968; Schuster and Dunnebacke, 1977; Volk and Maletz, 1985) or naturally occurring in human disease subjects (Brown et al., 1968; Gambetti and Gonatas, 1967; Raine and Field, 1968; Sung, 1980; Toper et al., 1980), initially led to a supposition that INRs are an aberrant nuclear inclusion formed as a result of a pathogenic process. A number of observations showing an increased occurrence of INRs with age seemed to support this view (David and Nathaniel, 1978; Feldman and Peters, 1972; Fiori, 1987; Knox et al., 1980). However, INRs are also present in apparently normal cells of both experimental and control subjects (Chandler and Willis, 1966; Clattenburg et al., 1972; de Estable-Puig and Estable-Puig, 1970; Feldman and Peters, 1972; Pinching and Powell, 1971;

Toper et al., 1980; Volk and Maletz, 1985; Woulfe et al., 2002). Most importantly, INRs can undergo cycles of formation and disassembly in response to physiological stimuli (Frink et al., 1978, discussed under "Insights into INR function"). Together this suggests that rather than being static, insoluble protein aggregates, INRs are dynamic structures more akin to nuclear bodies and must therefore have a normal nuclear function; which may nonetheless be affected under certain experimental or pathological conditions.

Insights into INR function

While a considerable body of knowledge has been accumulated regarding the morphology and distribution of INRs across the animal kingdom and within different tissues and cell types of a given organism, their functional and physiological significance remains a mystery.

Feldman and Peters (1972) proposed that INR formation is somehow related to the level of cellular activity. They drew on the reported observations in the nervous system of the highest frequency of INRs in the olfactory and cochlear nuclei, two sensory centers that are "never turned off" and keep receiving input even during the sleep portion of the sleep/wake cycle. Thus a cumulative stimulation effect in these neurons was suggested to be greater than for instance the visual or vestibular sensory centers. This idea of cumulative stimulation would also be consistent with the aforementioned age-related increase in INR frequency. Perhaps the most direct evidence in support of this hypothesis comes from the work of Seite et al. who have shown an increase in INR frequency in sympathetic neurons of the cat stellate ganglion in response to 15 minutes of pulsed electrical stimulation followed by a 10 minute repose (Seite et al., 1971b; Seite et al., 1973). The authors later showed that this effect can be replicated by elevated levels of the second messenger cAMP through administration of either non-metabolisable cAMP analogs or an inhibitor of phosphodiesterase (an enzyme responsible for cAMP breakdown) (Seite et al., 1977).

Induction of INR formation was also documented in relation to seasonal changes in the activity of woodchuck (*Marmot monax*) thyroid follicular cells (Frink et al., 1978). Thyroglobulin is actively synthesised for storage and release by the woodchuck thyroid follicular cells in the summer and fall. This is followed by a period of quiescence associated with winter hibernation. In the spring, as the animal comes out of hibernation the thyroid follicular cells actively release thyroglobulin that was stored during summer and fall. Ultrastructural examination of woodchuck thyroid glands collected in different seasons revealed that INRs are consistently present in thyroid follicular cells in the summer during the peak of cellular activity. INRs were also there, albeit "infrequently", in the fall when cellular activity subsides. In contrast, INRs were never found in winter during a period of quiescence or in spring when thyroid follicular cells are actively secreting thyroglobulin that was stored over the previous summer and fall. This prompted Frink et al. to propose a relationship between INRs and the rate of protein synthesis (Frink et al., 1978). Protein synthesis itself, however, does not appear to be necessary for INR formation as upregulation of INR formation by electrical stimulation in cat sympathetic neurons was not impeded by treatment with an inhibitor of protein synthesis, cycloheximide (Seite et al., 1973). Moreover, INR formation was reportedly induced by cycloheximide treatment in rat supraoptic nucleus (SON) neurons (Lafarga et al., 1993). This also suggests that INRs can be assembled from pre-existing proteins since their formation does not require *de novo* protein synthesis.

Contrarily, there have also been reports suggesting an inverse relationship between INR formation and cellular activity. Ultrastructural investigation of neurons of the preoptic and suprachiasmic nuclei in rabbits post coitus revealed ultrastructural changes consistent with elevated neurosecretory activity in ~30% of neurons located near capillaries (Clattenburg et al., 1972). In control animals, INRs were found in 31 out of 83 (37.3%) and in 25 out of a 100 (25%)

neuronal nuclei in the preoptic and suprachiasmic nucleus respectively. Similar INR frequencies were found post coitus in preoptic (19 of 84 nuclei, or 22.6%) and suprachiasmic (20 of 68 nuclei, or 29.4%) nucleus neurons that did not show ultrastructural changes following coitus. In contrast none of the neurons showing signs of elevated neurosecretory activity post coitus contained INRs (0 out of 148 neurons examined). While INRs were found in neurons of the preoptic and suprachiasmic nuclei in both post coitus and control rabbits, the authors noted that INRs were never observed in the nuclei of neurons showing ultrastructural evidence of elevated neurosecretory activity post coitus (Clattenburg et al., 1972). Thus an inverse relationship between INR formation and secretory activity could be proposed in these hypothalamic neurons.

An inverse relationship has been reported also between the frequency of INRs among oxytocin producing magnocellular neurons of rat SON and their oxytocin secretory activity (Berciano et al., 2004). In these neurons INR frequency significantly declined from 48% in virgin rats to 37% after parturition, where oxytocin release is required to induce uterine wall contraction; and to 40% during lactation, when elevated oxytocin secretion stimulates prolactin release and milk production. In contrast, INR frequency significantly increased to 68% at weaning when oxytocin secretion drops to baseline (Berciano et al., 2004). In the same oxytocin producing neurons of rat SON, a potential link was also established between INR formation and cellular transcriptional activity. Hyperosmotic stress induced by intraperitoneal injection of hypertonic saline induced a 3 fold increase in transcriptional activity 24 hours after injection (Lafarga et al., 1998). This increase inversely correlated with INR formation resulting in a reduction in INR frequency from 29% at the 0 hour time point to 18% at 24 hours post-injection (Villagra et al., 2008). Conversly, direct pharmacological inhibition of transcription with actinomycin-D induced INR formation in oocytes of newt (*Triturus viridescens*) (Lane, 1969).

Thus a mechanistic link between transcriptional activity and INR formation could be proposed and merits further investigation.

Other functional correlates of INR formation include postnatal development (David and Nathaniel, 1978; Masurovsky et al., 1970); X-ray irradiation (de Estable-Puig and Estable-Puig, 1970) and MPTP treatment (Lamba et al., 2005; Tucker et al., 1986) although, no specific mechanism has been identified.

The existence of such a diverse and at times conflicting array of stimuli reported to affect INR formation in diverse experimental systems may suggest that INRs have evolved to serve distinct physiological functions in different tissues and cell types.

Contemporary tools for INR research.

As mentioned above, INRs are believed to be composed mainly of protein. Their specific protein composition, however, remains largely unknown. There have been no reports of INR isolation and purification. Consequently, in situ labelling of INRs with target specific probes such as antibodies or oligonucleotide chains is currently the only source of insight into INR composition. In 2000, Woulfe et al. described the first immunohistochemical marker of INRs and used this to describe the topographic distribution of INRs in human brains. The authors used a monoclonal antibody, SDL.3D10, raised against a synthetic peptide corresponding to an eight amino acid carboxy-terminus epitope of class III β-tubulin (Woulfe and Munoz, 2000). They later demonstrated equivalent staining of SDL.3D10 immunoreactive INRs with another antibody, a polyclonal antiserum raised against human glucocorticoid receptor (Santa Cruz, GR-P20) (Woulfe et al., 2002). This type of SDL.3D10/GR-P20 immunoreactive INR heretofore will be referred to as SDL-INR.

The discovery of specific immunological INR markers provided a powerful tool for INR research that allowed for both INR quantification and co-localization studies of INRs with other target proteins. For instance, SDL-INRs were shown to be specifically and markedly diminished in Alzheimer's disease temporal cortex relative to age matched controls or subjects with another progressive neurodegenerative disorder, dementia with Lewy bodies (Woulfe et al., 2002). An increase in SDL-INR formation was demonstrated in dopaminergic neurons of substantia nigra (SN) in the MPTP-induced mouse model of Parkinson's disease (Lamba et al., 2005). In human substantia nigra, double immunofluorescence experiments have shown direct, non-random spatial interactions between SDL-INRs and ubiquitin immunoreactive Marinesco bodies. Interestingly, in human SN dopaminergic neurons ~30% of SDL-INRs themselves showed strong ubiquitin immunoreactivity and ~20% were immunoreactive for the 20S proteasome (Woulfe et al., 2004). A large proportion of human pigmented neurons in the substantia nigra was found to contain SDL-INRs immunoreactive for the promyelocytic leukemia protein (PML). A subset of these INRs was found in direct contact with PML nuclear bodies and all PML immunoreactive INRs were also immunoreactive for another marker of PML bodies, the transcriptional co-activator CBP. Some PML immunoreactive INRs were also positive for acetylated histone H4, the small ubiquitin-like modifier 1 protein (SUMO-1), and a known PML interactor, the eukaryotic translation initiation factor eIF4E (Woulfe et al., 2004; Woulfe et al., 2007). Morphologically and immunohistochemically similar structures were later reported in nuclei of human supraoptic nucleus neurons (Villagra et al., 2005).

While SDL.3D10 and GR-P20 antisera are powerful tools for INR detection, our unpublished data suggest that neither class III β-tubulin nor glucocorticoid receptor themselves are *bona fide* INR constituents (Appendix). SDL-INRs failed to stain with a number of other class III β-tubulin and glucocorticoid receptor specific antisera as well as pan-β-tubulin

antibodies. In addition, INRs could still be detected with the GR-P20 antibodies in a mouse with a conditional brain-specific glucocorticoid receptor knock out (Appendix; Panel 1). Furthermore, in cells transfected with hemagglutinin tagged class III β-tubulin, the fusion protein was incorporated into the cellular microtubule network but failed to incorporate into SDL-INRs as evidenced by SDL.3D10 and anti-hemagglutinin double immunofluorescence staining (Appendix; Panel 2). Thus the identity of the core INR component(s), including that/those immunoreactive for class III beta tubulin and glucocorticoid receptor remains unknown.

The widespread distribution and apparently ubiquitous SDL.3D10 and GR-P20 immunoreactivity of INRs initially led to the supposition that INRs comprise a biochemically homogeneous class of nuclear bodies. In this scenario, SDL.3D10 and GR-P20 immunoreactive moieties were considered to be constitutively present while proteins such as PML or ubiquitin were recruited or shed depending on the functional state of the INR. This view was challenged in 2004 by Berciano and colleagues who reported intranuclear structures in rat supraoptic nucleus neurons that could be identified morphologically and ultrastructurally as INRs but did not immunostain with the SDL.3D10 antibody. Instead these structures were intensely immunoreactive for poly(A) binding protein nuclear 1 (PABPN1). Although both PABPN1 and SDL.3D10 immunoreactive INRs were present in rat SON, they displayed a differential and mutually exclusive distribution with PABPN1 immunoreactive INRs (PABPN1-INRs) confined to magnocellular oxytocinergic neurons and SDL-INRs found in parvocellular neurons (Berciano et al., 2004). This indicated that INRs may represent a family of morphologically homogeneous, yet biochemically diverse intranuclear structures that are differentially distributed among neurochemically and/or functionally distinct neuronal subpopulations.

Hypotheses.

Despite the mounting evidence suggesting the importance of INRs as a functional nuclear compartment, few investigations focussed directly on INRs. To fill this gap in the understanding of nuclear architecture, I elected to make the INR phenomenon the central focus of my thesis project. Based on the available literature, I generated the following hypotheses:

1) Given the dynamic nature of INRs, I hypothesized that their expression is regulated and is linked to the functional or physiological state of the cells and tissues harbouring this nuclear body.
2) Numerous reports documenting INRs under both pathological conditions and in normal tissue raised the question of whether INR expression is affected in disease. A previous report from our laboratory strongly suggested specific involvement of SDL-INRs in the pathogenesis of Alzheimer's disease. This led me to hypothesize that SDL-INR expression would also be altered in other pathological conditions.
3) The expression of SDL-INRs in the human brain is widespread yet stereotypically defined. PABPN1-INRs were also shown to display a stereotypical CNS topography that was confined to a specific neurochemically defined neuronal subpopulation. In addition, PABPN1-INRs were reported to be negative for the SDL-INR marker, the SDL.3D10 antibody. This suggested that they represent an INR subtype that is biochemically distinct from SDL-INRs. I therefore hypothesized that there may be additional biochemically distinct INR subtypes that exhibit selective, INR subtype-specific localization to stereotypically and possibly neurochemically defined neuronal populations.

Experimental approach.

One of the most obvious corollaries of the first hypothesis is that there must be specific identifiable signalling pathways involved in the regulation of INR expression. The current rudimentary state of knowledge with regard to INRs, particularly with respect to their specific protein composition and functional significance, precluded the possibility of mechanistic studies or of postulating a hypothesis as to a specific pathway associated with INR regulation. Correlative studies aimed at the identification of broad physiological regulatory pathways associated with regulation of INR formation were, therefore, carried out as a logical first step to establish an experimental framework for subsequent studies interrogating more proximate downstream regulators. Building on this approach should eventually shed light on the functional significance, mechanistic aspects of action and specific protein composition of INRs.
Given the multitude of reported organisms and anatomical sites containing INRs as well as the apparently experimental model-dependent physiological aspects of their regulation and protein composition, the choice of model for INR research was crucial. INRs have been reported primarily in neurons and only occasionally in other cell types. However, the poor accessibility for experimental manipulation, the sheer complexity and heterogeneity of the central nervous system, and the lack of a reliable neuronal cell line which expressed INRs rendered the nervous system an unattractive model system in which to study INR regulation. To carry out these studies, it was imperative to employ a simpler, more functionally homogeneous model system. I found this in the form of the pancreatic β-cell model of INR expression.

INRs of the endocrine pancreas, first reported in mouse by Lennart Boquist in 1969 (Boquist, 1969), presented several advantages over the neuronal model. Pancreatic endocrine tissue is anatomically segregated from exocrine tissue into islets of Langerhans. It is relatively easy to isolate and purify to a considerable degree. There are only five principal cell types and

these can be easily differentiated by immunohistochemical staining methods. These are the glucagon producing α-cells, insulin producing β-cells, somatostatin producing δ-cells, pancreatic polypeptide producing γ-cells, and newly discovered ghrelin producing ε-cells (Wierup et al., 2002). Of these, insulin producing β-cells have the highest proportion of INRs and form the bulk of islet cell mass. Thus, pancreatic β-cells represent a relatively abundant, fairly homogeneous and accessible source of INRs. Most importantly, many physiological and molecular aspects of pancreatic β-cell regulation and function have been elucidated and a number of well-established experimental manipulations and animal models of human metabolic syndrome involving altered β-cell function are available (Islam and Loots du, 2009; Wajchenberg, 2007). The β-cell INR model was therefore selected for the study of INR regulation and its relevance in the context of disease pathogenesis.

Our first objective was to determine whether the INRs that had been described by electron microscopy in mouse islet cells were immunohistochemically equivalent to the SDL-INRs that we had described in human brain and whether SDL-INRs were present in human pancreatic islets. Since INRs had not been previously reported in human β cells, this was important also in order to establish the relevance of studying mouse β-cell INRs to human β-cell biology and the disruption of β-cell function associated with human metabolic syndrome. This work is described in chapter 1 of this thesis.

To establish correlations and signalling pathways linking INR formation and β-cell function, as would be predicted from the first hypothesis proposed in the "Hypotheses" section above, a mouse model of altered β-cell energy and metabolism regulation was examined. Specifically, an adult β-cell-specific Lkb1 kinase knock out mouse model featuring altered β-cell polarity and insulin secretory function was employed to look for a correlation between β-cell structure, function and INR expression. This model was chosen because Lkb1 is a master

regulator of β-cell structure and function. Consequently, we reasoned that INR formation would be influenced by at least one, if not more, of its many downstream effectors. Subsequent studies could then interrogate each of the latter to narrow down the proximate molecular regulators of INR formation. Indeed, I specifically examined two of the downstream effectors of the Lkb1 knockout mouse phenotype for a potential role in the regulation of INR prevalence.

In order to validate my second hypothesis that SDL-INR expression would be altered under pathological conditions, I investigated β-cell INRs in two distinct mouse models of obesity related diabetes. Specifically, I looked for changes in INR prevalence induced by either a genetic knock out of leptin; or by maintenance on a high fat diet - both conditions mimicking increased body weight, peripheral tissue insulin resistance and compensatory hyperinsulinemia associated with the early onset stages of the human metabolic syndrome. This part of the project is described in chapter 2 of this thesis.

Finally we also looked to the current literature for new emerging clues that could help further our understanding of INR biology. While perusing the current literature pertaining to INRs, we came across a report of the cellular and topographic pattern of distribution of huntingtin associated protein 1 (Hap1) in the mouse brain (Gutekunst et al., 1998). Remarkably, in some neurons, Hap1 immunoreactivity was localized to intranuclear rod-shaped structures. In order to determine whether Hap1 immunoreactivity was a feature of SDL-INRs or represented a marker of a novel INR subtype, in accordance with my third hypothesis, I examined whether INRs we observed using our SDL.3D10 and GR-P20 antibodies were also immunoreactive for Hap1 using commercially available antibodies. While I was not able to detect the Hap1 immunoreactive INRs, I discovered a new subtype of INR that was instead immunoreactive for another huntingtin associated protein, the 40 kDa huntingtin associated protein (Hap40). Hap40 immunoreactive INRs (Hap40-INRs) were not immunoreactive for the SDL.3D10 antibody and had a

topographically distinct pattern of distribution with selective localization to certain neurochemically defined neuronal populations, as was predicted by the third hypothesis. The discovery and characterization of this new INR subtype is described in chapter 3 of this thesis.

Chapter 1.

The manuscript contained in this chapter had been published in the peer-reviewed journal *Pancreas*.

Statement of student's contribution:

Pavel Milman contributed significantly to this co-authored paper. The fluorescence double-labelling immunohistochemistry and microscopic analysis and quantification for this study had just begun at the time of Pavel's arrival in Dr. Woulfe's lab. This represented his introduction to this laboratory and, during this time, he followed Ms. Prichett, Dr. Woulfe's technician, closely to learn to perform double labelling immunofluorescence staining, image acquisition and analysis, and subsequently performed some of the staining and imaging used in preparation of this paper. Finally, while he was not the primary contributor to writing of this manuscript, he contributed to the data analysis, the formulation of ideas expressed in the Discussion and to the final editing of this manuscript.

John Woulfe,

Pavel Milman.

Foreword:

Unpublished results from our lab as well as previous electron microscopy studies have demonstrated the presence of INRs in mouse endocrine pancreas. INRs however had not been previously investigated in human pancreatic tissue. The relevance of INRs to the nuclear architecture of the human pancreatic endocrine cells was investigated in this chapter.

Intranuclear Rodlets in Human Pancreatic Islet Cells

Wendy Prichett, BSc(Hon)*, Pavel Milman, MSc†, Jeff Gagnon, BSc†, David G. Munoz, MD‡, and John Woulfe, MD, PhD *†§||

Objectives: Intranuclear rodlets (INRs) are rod-shaped intranuclear inclusions that we have described in neurons of the human brain. We recently identified these structures in pancreatic islet cells. The objectives of this study are to describe the light microscopic features and cellular pattern of distribution of INRs in human pancreatic islet cells.

Methods: Double immunofluorescence staining was performed on 5 human pancreatic tissue samples for the detection of class III β-tubulin (C3T) to detect INRs and for promyelocytic leukemia (PML) protein to examine the relationship between PML and INRs.

Results: Intranuclear rodlets were detected in 22.99% of pancreatic β-cells compared with only 3.11%, 1.80%, and 1.60% of α, δ, and PP cells, respectively. Twenty-four percent of C3T-immunoreactive INRs showed partial or complete immunoreactivity for PML. Promyelocytic leukemia staining within the nuclei of β cells was confined to INRs and was not present in the

typical PML bodies present in other cell types. Spatially, PML and C3T staining of islet cell INRs appeared to be mutually exclusive within individual INRs.

Conclusions: Intranuclear rodlets are present within the nuclei of pancreatic islet cells, where they reside predominantly but not exclusively in β cells. Immunoreactivity of β-cell INRs for PML suggests that the functional significance of INRs may be related to that of PML and/or PML bodies. Conversely, the exclusive localization of PML staining to INRs in β cells indicates that PML's function in β cells is selectively associated with INRs. The mutually exclusive pattern of PML and C3T staining suggests dynamic interactions between these 2 proteins in β-cell INRs. In light of evidence for the involvement of INRs and of PML bodies in disease, it will be of interest to investigate these structures in animal models of diabetes and in human diabetes.

Key Words: class III β tubulin, intranuclear rodlet, pancreatic β cell, pancreatic islet cell, promyelocytic leukemia protein, PML body

Received for publication November 27, 2006; accepted April 3, 2007.

From the *Centre for Cancer Therapeutics, The Ottawa Health Research Institute, Ottawa; †Department of Biochemistry, Microbiology, and Immunology, University of Ottawa, Ottawa; ‡Department of Pathology, St Michael's Hospital, Toronto; §Department of Pathology, The Ottawa Hospital, Ottawa; ||Department of Laboratory Medicine, University of Ottawa, Ottawa.

Financial support for this study was provided by The Alzheimer Society of Canada and The Parkinson Society of Canada.

(Pancreas 2007;35:207Y211)

INTRODUCTION

There is growing appreciation for the functional significance of nuclear substructure and a growing number of nuclear structures or nuclear bodies have been described[1,3]. In addition to nucleoli, these structures include promyelocytic leukemia (PML) bodies, Cajal bodies, nuclear speckles, Gemini of coiled bodies (Gems), and others. Although specific functional roles have been, with various degrees of certainty, assigned to some nuclear structures, such as assembly of transcriptosomes and splicosomes for Cajal bodies[4] or pre-messenger RNA processing for cleavage bodies[5] and nuclear speckles[6] functional niches for others remain more ambiguous. The significance of this nuclear substructure in pancreatic islet cells has not been investigated. Intranuclear rodlets (INRs) have been included in the family of nuclear bodies[3]. These rod-shaped intranuclear structures in neurons were known to the classical anatomists[7-9] and have been referred to as "rodlets of Roncoroni". Subsequent ultrastructural studies revealed that they consist of parallel arrays of closely packed filaments[10-16]. With the exception of rare studies linking the formation of INRs to aging[17], neuronal electrical activity[18], or cyclic adenosine monophosphate signaling[19], the functional and/or pathological significance of these structures remains unknown.

We demonstrated that these neuronal INRs are immunoreactive for the neuron-specific cytoskeletal protein class III β tubulin (C3T)[20]. This provided a contemporary tool to study the functional and/or pathological significance of INRs. We have since provided evidence that INRs have functional and pathological significance in the nervous system. They show a widespread and anatomically heterogeneous pattern of distribution in the brain[20]. A proportion of INRs in the human brain are immunoreactive for PML protein, the signature constituent protein of PML nuclear bodies[21,22]. Thus, INRs are related to PML bodies. In some areas such as the substantia

nigra, they display immunostaining for ubiquitin-proteasome system components as well as for transcriptionally relevant proteins including the transcriptional regulator CBP and acetylated histone H4, a marker for transcriptionally active chromatin[22]. This latter finding suggests that they may be involved in transcriptional regulation, as has been proposed for INRs in other brain regions, such as the supraoptic nucleus[23]. We have demonstrated that these structures may have pathological significance because they are markedly reduced in the cerebral cortex of patients with Alzheimer disease[24] and are increased in the substantia nigra of mice treated with the parkinsonism-inducing neurotoxin 1-methyl-4-phenyl-1,2,3,6tetrahydropyridine[25].

Intranuclear rods have been described in nondiseased pancreatic islet cells in ultrastructural studies of mice[26] and birds[27,28]. In mice, these structures were confined to β cells and were not encountered in α cells[26]. We were interested to determine whether the INRs described in ultrastructural studies of pancreatic islet cells were equivalent to the C3T-immunoreactive INRs we described in neurons. We also investigate whether there is a cell-type specific expression of INRs among pancreatic α, β, δ, and PP cells synthesizing glucagon, insulin, somatostatin, and pancreatic polypeptide, respectively, and, by analogy with neurons, whether pancreatic INRs are associated with PML or PML bodies.

MATERIALS AND METHODS

Immunohistochemistry

Formalin-fixed, paraffin-embedded blocks of human pancreas from 5 subjects who underwent Whipple procedure for resection of pancreatic adenocarcinoma (3 men and 2 women; mean age, 73 years) were examined. Four micrometer-thick sections were cut and examined by double immunofluorescence labeling. Sections were incubated for 24 hours in a mixture of anti-C3T (mouse monoclonal, 1:100; Sigma, St Louis, Mo) and an antibody to one of the following: rabbit polyclonal anti-insulin (1:200; Santa Cruz Biotechnologies, Santa Cruz, Calif), goat polyclonal anti-glucagon (1:50; Santa Cruz Biotechnologies), rabbit poly-clonal anti-somatostatin (1:800; DAKO Cytomation, Carpinteria, Calif), rabbit polyclonal anti-pancreatic polypeptide (1:2000; DAKO Cytomation), or goat polyclonal anti-PML antibody (1:50; Santa Cruz Biotechnologies). The sections were then rinsed and incubated in the dark for 45 minutes in a mixture of AlexaFluor 488 chicken antigoat IgG (H + L) (1:150; emission peak, 519 nm; Molecular Probes, Eugene, Ore) and AlexaFluor 594 donkey anti-mouse IgG (H + L) (1:150; emission peak, 613 nm; Molecular Probes) (C3T/glucagon) or AlexaFluor 488 goat anti-mouse IgG (H + L) (1:150; emission peak, 519 nm; Molecular Probes) and AlexaFluor 594 donkey anti-rabbit IgG (H + L) (1:150; emission peak, 613 nm; Molecular Probes) (C3T/insulin, C3T/somatostatin, and C3T/PP). Sections were coverslipped using Vectashield Mounting Medium containing 1.5 µg/mL 4'-6-diamidino-2-phenylindole (DAPI) as a nuclear counterstain. Sections were examined using a Zeiss Axioplan II fluorescence microscope (Carl Zeiss Microscopy, Jena, Germany) with attached AxioCam digital camera. Manual counts of insulin, glucagon, somatostatin, and PP-immunoreactive cells were performed, and the proportion of INRs in each cell type was calculated. Only cells in which the DAPI-stained nucleus was visible were counted. For estimates

of the proportion of PML-immunoreactive INRs, 100 C3T-immunoreactive INRs from each case were selected at random and assessed for PML immunostaining in double-stained sections.

RESULTS

Intranuclear Rodlets Predominate in Pancreatic β cells

Immunoflurescence analysis of double-immunostained sections of formalin-fixed, paraffin-embedded human pancreas stained for C3T revealed immunoreactive INRs in cells in islets of Langerhans including α, β, δ, and PP cells (Fig. 1). These inclusions were predominantly rod- or needle-shaped, although dot-like forms were also identified. The former were straight or curved, and many appeared to appose the nuclear envelope at one or both ends. Figure 2 shows the proportion of α, β, δ, and PP cells containing INRs in each of the 5 cases. Intranuclear rodlets were clearly predominant in pancreatic β cells with an overall mean proportion of 22.99% containing INRs compared with a mean of only 3.11%, 1.80%, and 1.60% in α, δ, and PP cells, respectively. However, there was wide inter-individual variation. Ranges were from 4.41% to 30.22% in β cells, 0.69% to 5.80% in α cells, 0% to 3% in δ cells, and 0% to 5% in PP cells.

Intranuclear Rodlets Are Immunoreactive for PML

Most cells in the pancreas, including exocrine cells, ductal cells, endothelial cells, and even carcinoma cells (where present in the section) contained the typical array of 10 to 30 randomly distributed, roughly spherical, 0.2-to 1-μm PML bodies (Fig. 3). In pancreatic islet cells, however, this conventional pattern was not observed. Instead, where present, PML immunoreactivity was confined to rod-shaped or, occasionally, dot-shaped structures that corresponded, on C3T staining, to INRs. Thus, an average of 24% of C3T immunoreactive INRs (range, 10-41%) showed complete or partial immunoreactivity for PML protein. Interestingly, C3T and PML labeling of INRs appeared to be mutually exclusive, whereby PML-positive sections were C3T-negative and vice versa. This mutual exclusivity was highlighted in the case

with the lowest frequency of C3T-immunoreactive INRs (6.48%). Forty-one percent of C3T-positive INRs, which were difficult to find, showed PML staining. Conversely, only 7% of PML-immunoreactive INRs in this case showed C3T staining, indicating that, unlike the other 4 cases in which C3T-positive/PML-negative INRs predominated, the opposite was true in this case.

Figure 1. Intranuclear rodlets in human pancreatic islet B cells.

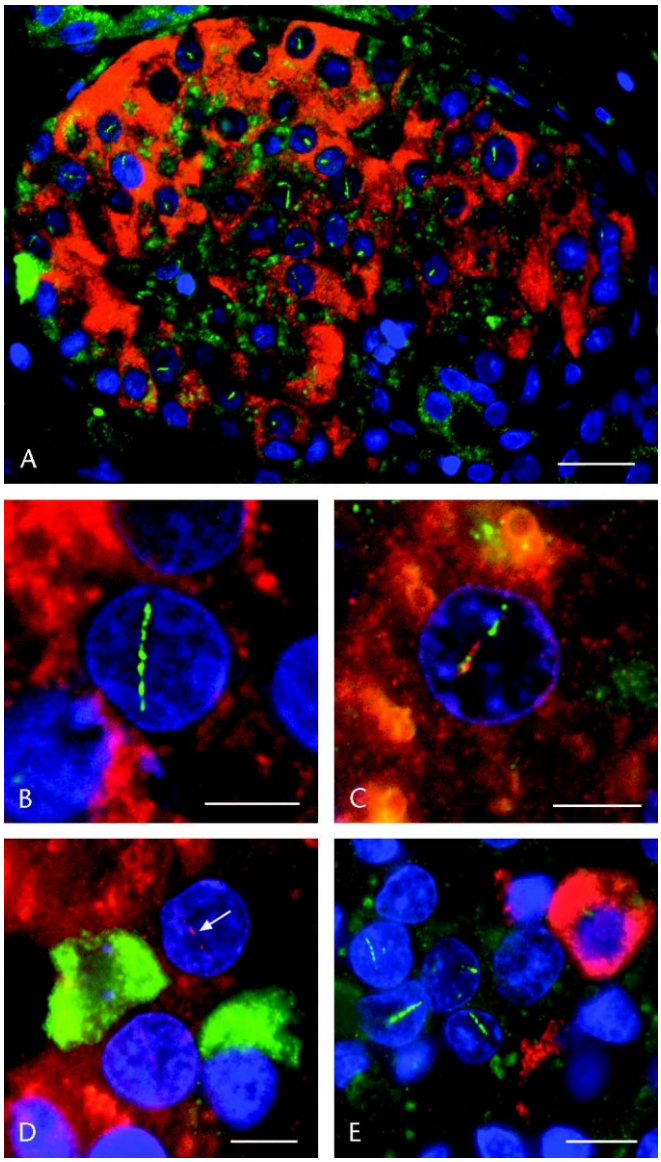

Legend to Figure 1. Intranuclear rodlets in human pancreatic islet B cells. C3T-immunoreactive (IR) INRs (green) in insulin-IR B cells (red) seen at low (A) and high power (B). C3T-IR INR showing partial PML-IR (C). C3T-IR INRs (D, red with arrow; E, green) in nuclei of cells negative for glucagon (D, green) and somatostatin (E, red). Nuclei counterstained with DAPI (blue). Bars = 20 μm (A), 5 μm (B-D), and 10 μm (E).

Figure 2. Intranuclear rodlets predominate in human B cells.

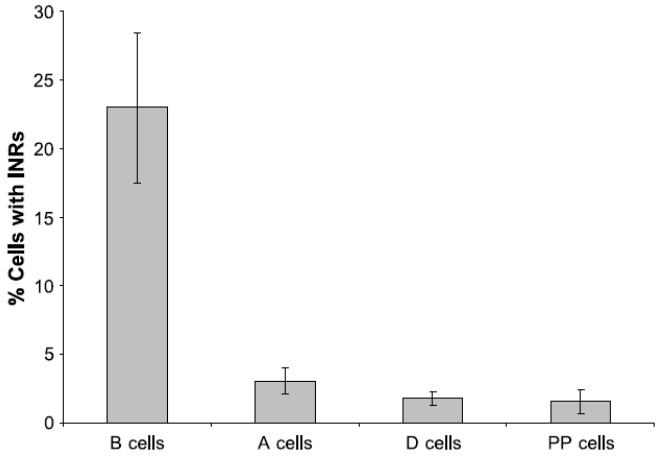

Legend to Figure 2. Intranuclear rodlets predominate in human B cells.
Mean percentage of INR-containing insulin-positive B, glucagon-positive A, somatostatin-positive D, and pancreatic polypeptide Y positive PP cells in 5 human pancreatic samples. Error bars show the SEM.

Figure 3. Proportion of B-cell INRs immunoreactive for PML.

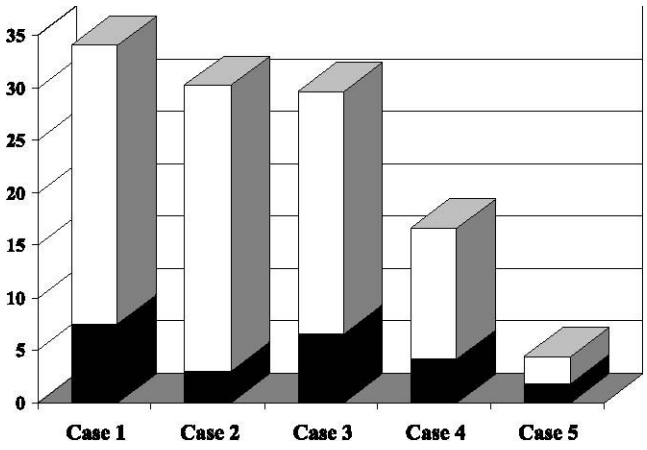

Legend to Figure 3. Proportion of B-cell INRs immunoreactive for PML.
Each bar shows the percentage of B cells containing INRs for each of the 5 cases. The black bar in each case denotes the proportion of those INRs that showed partial immunoreactivity for PML protein.

DISCUSSION

This descriptive study confirms earlier electron microscopic investigations revealing the presence of rod or needle-shaped intranuclear inclusions in pancreatic β cells in vivo from a variety of species[26-28]. By virtue of their immunoreactivity for C3T, these structures are equivalent to the INRs that we have described in neurons of normal human brain.[20] The pancreatic tissue used in this study was taken from our archive of formalin-fixed, paraffin-embedded surgical specimens. There are several advantages to using surgical material rather than archived postmortem material. Chief among these is the absence of substantial autolysis in our specimens, a common finding in postmortem pancreas. Moreover, using surgical material precludes the possibility that any of the changes that we described are consequent upon postmortem effects. However, we cannot exclude the possibility that the presence of adenocarcinoma in our samples influenced the frequency of pancreatic islet cell INRs. However, the lack of an obvious regional gradient in INR frequencies in islet cells with respect to proximity to the tumour argues against this possibility. Moreover, the frequency of INRs, at least in β cells, is consistent with what we have seen in the islets of mice in our preliminary studies.

The human adult endocrine pancreas consists of 4 hormonally distinct cell types: α, β, δ, and PP cells synthesizing glucagon, insulin, somatostatin, and pancreatic polypeptide, respectively.[29] Consistent with a previous ultrastructural study,[26] we have demonstrated that INRs predominate in insulin-immunoreactive β cells. However, they were identified, albeit rarely, in the other cell types as well. This suggests that the functional significance of these structures is not exclusively related to insulin secretion or glucose metabolism but instead to other aspects of islet cell function shared among the various cell types but exaggerated in β cells. The functional significance of INRs in pancreatic islet cells is uncertain. In neurons, recent studies have

demonstrated an inverse correlation between the formation of INRs composed of polyadenylation binding protein nuclear 1 and the level of activity of neurosecretory neurons in the rat supraoptic nucleus.[30] The identification of INRs in pancreatic islet cells will offer a novel tool with which to investigate the relationship between INR formation and cellular secretory activity.

The immunostaining of a proportion of islet cell INRs with PML is consistent with our studies in human brain demonstrating PML immunoreactivity of a smaller proportion of neuronal INRs.[21] Interestingly, PML immunostaining in pancreatic islet cells was unusual in that it was confined to INRs. This indicates that the function of PML in pancreatic islet cells is selectively related in some way to that of INRs. Moreover, the mutual exclusivity of PML and C3T immunostaining suggests a dynamic equilibrium between these 2 protein constituents of INRs. Is it possible to deduce the functional significance of INRs in pancreatic β cells based on what is known about the role of PML bodies? Promyelocytic leukemia bodies have been implicated in a wide variety of nuclear functions, including transcription, DNA repair, viral defense, stress, cell cycle regulation, alternative lengthening of telomeres, proteolysis, and apoptosis, and there is still vigorous debate about their true biological function(s).[31] They are defined by the presence of PML protein, first identified as the fusion partner with retinoic acid receptor α in the t(15,17) translocation that causes acute PML.[32] Although PML is the defining protein of PML bodies and is necessary for their formation, more than 50 other proteins have been found to be transiently or constitutively associated with them.[31,33,34] One of the more convincing postulated functions, based on the compositional heterogeneity of PML bodies, is as a nuclear depot for several proteins[33,35] that are recruited and released in a regulated manner. Such a depot function could be useful to facilitate the rapid release of stored proteins when they are required but would otherwise keep them segregated to prevent adverse interactions within the cell. Importantly, the presence of proteosomes next to some PML bodies is consistent with a role for PML bodies in intranuclear

proteolysis. It would suggest that in some circumstances, there is proteolytic elimination of the proteins stored in the PML nuclear depot.[36] It is tempting to speculate that PML-positive/C3T-negative areas of INRs reflect successful PML-mediated proteolysis of the C3T-immunoreactive protein.

Immunoreactivity of pancreatic INRs for C3T is interesting in this respect. Increased insulin secretion in pancreatic β cells is correlated with changes in the concentrations of polymerized relative to unpolymerized tubulin. Thus, in resting β cells, only 23% of tubulin is in the form of microtubules, increasing to 36% on stimulation.[37-39] The cellular localization of this large unpolymerized pool remains unknown.[39] Intranuclear rodlets may represent an aggregate of unpolymerized β-tubulin localizing to the nuclear compartment and available for incorporation into microtubules on glucose stimulation. A major problem with this model concerns the identity of the C3T-immunoreactive protein in INRs. Intranuclear rodlets are intensely immunoreactive using a single monoclonal antibody (clone SDL.310; Sigma) generated against the extreme c-terminal tail of the cytoskeletal protein C3T.[40] However, INRs fail to stain with several other monoclonal antibodies generated against isoform-specific epitopes of C3T as well as with monoclonal and polyclonal antibodies against β-tubulin epitopes shared among the different isoforms. Thus, the identity of the C3T-immunoreactive protein in INRs remains to be identified. It may be a complex polymeric assembly of full-length, truncated, misfolded, or posttranslationally modified C3T in which the epitopes recognized by other antibodies are hidden. Alternatively, it may be a nonrelated cross-reacting protein. Proteomic studies are underway to address these possibilities.

Both PML nuclear bodies and INRs have been implicated in disease states. We have demonstrated that INRs have pathological significance because they are markedly reduced in the cerebral cortex of patients with Alzheimer disease[24] and are increased in the substantia nigra of

mice treated with the parkinsonism-inducing neurotoxin 1-methyl-4-phenyl-1,2,3,6-tetrahydropyridine.[25] Disruption of PML bodies has been described in a variety of disease processes, including virus infections, acute PML, and neurodegenerative disorders, specifically, the polyglutamine repeat diseases.[41] These diseases are characterized pathologically by the presence of ubiquitinated intranuclear inclusions containing mutant misfolded polyglutamine protein. Promyelocytic leukemia and other PML body proteins redistribute to these inclusions with the disruption of PML bodies.[42] It has been proposed that the consequent compromise of PML body function may have a role in disease pathogenesis. In this context, it is conceivable that the presence of PML in β-cell INRs is actually detrimental and that this distinctive feature of pancreatic β cells is one of the factors that render them selectively vulnerable to a variety of cellular insults. It will be interesting to determine whether PML and its association with INRs in pancreatic islet cells have a role in the pathogenesis of diabetes.

ACKNOWLEDGMENT

The authors acknowledge the support of the Ottawa Parkinson's Disease Research Consortium.

REFERENCES

1. Handwerger KE, Gall JG. Subnuclear organelles: new insights into form and function. Trends Cell Biol. 2006;16:19Y26.

2. Lamond AI, Sleeman JE. Nuclear substructure and dynamics. Curr Biol. 2003;13:R825YR828.

3. Berciano MT, Villagra NT, Pena E, et al. Structural and functional compartmentalization of the cell nucleus in supraoptic neurons. Microsc Res Tech. 2002;56:132Y142.

4. Gall JG. Cajal bodies: the first 100 years. Annu Rev Cell Dev Biol. 2000;16:273Y300.

5. Schul W, van Der Kraan I, Matera AG, et al. Nuclear domains enriched in RNA 3¶-processing factors associate with coiled bodies and histone genes in a cell cycleYdependent manner. Mol Biol Cell. 1999;10: 3815Y3824.

6. Fu XD, Maniatis T. The 35-kDa mammalian splicing factor SC35 mediates specific interactions between U1 and U2 small nuclear ribonucleoprotein particles at the 3¶ splice site. Proc Natl Acad Sci U S A. 1992;89:1725Y1729.

7. Roncoroni L. Su un nuovo reperto nel nucleo delle cellule nervose. Arch Psychiatr. 1895;16:477.

8. Mann G. Histological changes induced in sympathetic, motor, and sensory nerve cells by functional activity. J Anat Physiol. 1894;29: 100Y108.

9. Cajal S. Histologie du Systeme Nerveux de l'Homme et des Vertebres. Vols. I and II. Paris: Maloine; 1909Y1911.

10. Siegesmund KA, Dutta CR, Fox CA. The ultrastructure of the intranuclear rodlet in certain nerve cells. J Anat. 1964;98:93Y97.

11. Willey TJ, Schultz RL. Intranuclear inclusions in neurons of the cat primary olfactory system. Brain Res. 1971;29:31Y45. 12. Clattenburg RE, Singh RP, Montemurro DG. Intranuclear filamentous inclusions in neurons of the rabbit hypothalamus. J Ultrastruct Res. 1972;39:549Y555.

13. Lafarga M, Palacios G. Intranuclear rodlets in retrochiasmatic area neurons of the hypothalamus of the rat. Experientia. 1977;33:1368Y1369.

14. Lafarga M, Palacios G. Nuclear inclusions in paraventricular nucleus neurons of the rat hypothalamus. Cell Tissue Res. 1979;203:223Y229.

15. Masurovsky EB, Benitez HH, Kim SU, et al. Origin, development, and nature of intranuclear rodlets and associated bodies in chicken sympathetic neurons. J Cell Biol. 1970;44:172Y191.

16. Seite R, Vuillet-Luciani J, Zerbib R, et al. Thee-dimensional organization of tubular and filamentous nuclear inclusions and associated structures in sympathetic neurons as revealed by serial sections and tilting experiments. J Ultrastruct Res. 1979;69:211Y231.

17. Field EJ, Peat A. Intranuclear inclusions in neurones and glia: a study in the ageing mouse. Gerontologia. 1971;17:129Y138.

18. Seite R, Mei N, Vuillet-Luciani J. Effect of electrical stimulation on nuclear microfilaments and microtubules of sympathetic neurons submitted to cycloheximide. Brain Res. 1973;50:419Y423.

19. Seite R, Leonetti J, Luciani-Vullet J, et al. Cyclic AMP and ultrastructural organization of the nerve cell nucleus: stimulation of nuclear microtubules and microfilaments assembly in sympathetic neurons. Brain Res. 1977;124:41Y51.

20. Woulfe J, Munoz D. Tubulin immunoreactive neuronal intranuclear inclusions in the human brain. Neuropathol Appl Neurobiol. 2000;26:161Y171.

21. Woulfe J, Gray D, Prichett-Pejic W, et al. Intranuclear rodlets in the substantia nigra: interactions with marinesco bodies, ubiquitin, and promyelocytic leukemia protein. J Neuropathol Exp Neurol. 2004;63:1200Y1207.

22. Woulfe J. PML-immunoreactive neuronal intranuclear rodlets in the human brain. Neuropathol Appl Neurobiol. 2007;33:56Y66.

23. Villagra NT, Navascues J, Casafont I, et al. The PML-nuclear inclusion of human supraoptic neurons: a new compartment with SUMO-1Y and ubiquitin-proteasomeYassociated domains. Neurobiol Dis. 2006;21: 181Y193.

24. Woulfe JM, Hammond R, Richardson B, et al. Reduction of neuronal intranuclear rodlets immunoreactive for tubulin and glucocorticoid receptor in Alzheimer's disease. Brain Pathol. 2002;12:300Y307.

25. Lamba W, Prichett W, Munoz D, et al. MPTP induces intranuclear rodlet formation in midbrain dopaminergic neurons. Brain Res. 2005; 1066:86Y91.

26. Boquist L. Intranuclear rods in pancreatic islet beta-cells. J Cell Biol. 1969;43:377Y381.

27. Hoshino T. Occurrence of intranuclear protein inclusion bodies in the beta cells of the Langerhans' islets in chicks. Igaku To Seibutsugaku. 1969;78:193Y196.

28. Iwanaga T, Yamada J, Yamashita T, et al. Intranuclear filamentous inclusions in the gastro-entero-pancreatic (GEP) endocrine cells of birds. Cell Tissue Res. 1981;217:283Y288.

29. Kloppel G, In't Veld PA, Komminoth P, et al. The endocrine pancreas. In: Kovacs K, Asa SL, eds. Functional Endocrine Pathology. Oxford: Blackwell Scientific; 1998:415Y487.

30. Berciano MT, Villagra NT, Ojeda JL, et al. Oculopharyngeal muscular dystrophy-like nuclear inclusions are present in normal magnocellular neurosecretory neurons of the hypothalamus. Hum Mol Genet. 2004;13:829Y838.

31. Borden KL. Pondering the promyelocytic leukemia protein (PML) puzzle: possible functions for PML nuclear bodies. Mol Cell Biol. 2002;22:5259Y5269.

32. de The H, Lavau C, Marchio A, et al. The PML-RAR alpha fusion mRNA generated by the t(15;17) translocation in acute promyelocytic leukemia encodes a functionally altered RAR. Cell. 1991;66:675Y684.

33. Negorev D, Maul GG. Cellular proteins localized at and interacting within ND10/PML nuclear bodies/PODs suggest functions of a nuclear depot. Oncogene. 2001;20:7234Y7242.

34. Salomoni P, Pandolfi PP. The role of PML in tumor suppression. Cell. 2002;108:165Y170.

35. Maul GG, Negorev D, Bell P, et al. Review: properties and assembly mechanisms of ND10, PML bodies, or PODs. J Struct Biol. 2000;129:278Y287.

36. Lallemand-Breitenbach V, Zhu J, Puvion F, et al. Role of promyelocytic leukemia (PML) sumolation in nuclear body formation, 11S proteasome recruitment, and As2O3-induced PML or PML/retinoic acid receptor alpha degradation. J Exp Med. 2001; 193:1361Y1371.

37. Pipeleers DG, Pipeleers-Marichal MA, Kipnis DM. Microtubule assembly and the intracellular transport of secretory granules in pancreatic islets. Science. 1976;191:88Y90.

38. Pipeleers DG, Pipeleers-Marichal MA, Kipnis DM. Regulation of tubulin synthesis in islets of Langerhans. Proc Natl Acad Sci U S A. 1976; 73:3188Y3191.

39. Howell SL, Tyhurst M. Microtubules, microfilaments and insulin-secretion. Diabetologia. 1982;22:301Y308.

40. Banerjee A, Roach MC, Trcka P, et al. Increased microtubule assembly in bovine brain tubulin lacking the type III isotype of beta-tubulin. J Biol Chem. 1990;265:1794Y1799.

41. Matera AG. Nuclear bodies: multifaceted subdomains of the interchromatin space. Trends Cell Biol. 1999;9:302Y309.

42. Dovey CL, Varadaraj A, Wyllie AH, et al. Stress responses of PML nuclear domains are ablated by ataxin-1 and other nucleoprotein inclusions. J Pathol. 2004;203:877Y883.

Chapter 2.

The manuscript contained in this chapter had been published in the peer-reviewed journal of *Endocrine Pathology*.

Statement of student's contribution:

Data collection and analysis for this study was performed by Pavel Milman. LABKO mouse pancreatic tissue sections from a previously published study by Fu et al. 2009 were used in this study and were supplied by Accalia Fu and Robert Screaton. Accalia Fu assisted in sample collection from ob/ob mice and performed insulin ELISA for these mice. The manuscript was drafted by Pavel Milman and edited jointly by all four authors.

John Woulfe,

Pavel Milman.

Foreword:

Having confirmed the immunoreactivity of pancreatic INRs for the SDL.3D10 marker in human tissue, as a strategic approach to elucidating INR biology, I addressed candidate cellular pathways involved in the regulation of formation and disassembly of INRs in mouse pancreatic beta cells. To do this, I started with a global regulator of β-cell metabolism, the Lkb-1 kinase, in order to cast as wide a net as possible in search of candidates for the INR related regulatory pathways. Subsequent analysis was initiated to narrow down more specifically the pathway involved in INR regulation.

Pertinent to my second hypothesis, the second goal in this study was to see whether INRs are affected and hence potentially involved in the development of the metabolic syndrome associated with beta-cell dysfunction.

Depletion of Intranuclear Rodlets in Mouse Models of Diabetes

Pavel Milman & Accalia Fu & Robert A. Screaton &John M. Woulfe

Keywords Diabetes . Pancreatic islet . Beta cell . Insulin . Leptin . Intranuclear rodlet

P. Milman : A. Fu : J. M. Woulfe: Department of Biochemistry, Microbiology, and Immunology, University of Ottawa, Ottawa, Ontario, Canada

P. Milman : J. M. Woulfe: Cancer Therapeutics Program, Ottawa Hospital Research Institute, Ottawa, Ontario, Canada

A. Fu : R. A. Screaton: Children's Hospital of Eastern Ontario Research Institute, Ottawa, Ontario, Canada

J. M. Woulfe: Department of Pathology and Laboratory Medicine, University of Ottawa, Ottawa, Ontario, Canada

R. A. Screaton: Department of Pediatrics, University of Ottawa, Ottawa, Ontario, Canada R. A. Screaton: Department of Cellular and Molecular Medicine, University of Ottawa, Ottawa, Ontario, Canada

J. M. Woulfe: Department of Pathology, The Ottawa Hospital, Civic Campus, Ottawa, Ontario, Canada

Endocr Pathol

DOI 10.1007/s12022-010-9136-5

Abstract.

Intranuclear rodlets (INRs) are structures present within the nuclei of human insulin-secreting beta cells of the endocrine pancreas. Their physiological significance, and whether they are altered in disease, is unknown. In the present study, the proportion of pancreatic beta cells containing INRs was examined in mouse models of type II diabetes and in a model with improved beta cell function. To gain insights into the molecular regulators of INR formation, mice with a conditional adult beta cell-specific knockout of the serine/threonine protein kinase Lkb1 (Lkb1 adult beta cell knockout (LABKO) mice) were studied. To investigate INR changes in a pathophysiological context, beta cell INRs were examined in two models of human metabolic syndrome: (1) mice maintained on a high-fat diet and (2) leptin-deficient ob/ob mice. The proportion of beta cells containing INRs was significantly reduced in LABKO mice. This reduction was not mediated by two key downstream effectors of Lkb1, mTor and Mark2. High-fat diet regimen reduced beta cell INR frequency by more than 40%, and leptin-deficient ob/ob mice exhibited a dramatically (19-fold) reduced INR frequency relative to wild-type mice. Taken together, our results support the view that INR formation in pancreatic beta cells is a dynamic and regulated process. The substantial depletion of beta cell INRs in LABKO and diabetic mice suggests their relationship to beta cell function and potential involvement in diabetes pathogenesis.

Introduction.

There is increasing evidence that dysfunction of insulin secreting beta cells in the pancreatic islets of Langerhans plays a primary role in the pathogenesis of type II diabetes (T2D) [1]. Beta cells are archetypal metabolic sensors and critical regulators of blood glucose homeostasis. The precise cellular mechanisms through which they achieve this and the factors underlying their failure in diabetes remain to be completely elucidated [1]. The study of beta cell morphology has contributed substantially to our understanding of beta cell function and dysfunction. We recently described the existence of intranuclear rodlets (INRs) in human endocrine pancreas [2]. These structures, which we originally identified in neurons [3], are distinct, nuclear, rod-shaped filamentous structures that stain intensely with a monoclonal antibody generated against the neuron-specific cytoskeletal protein class III beta tubulin (C3T). In pancreas, INRs are found predominantly in beta cells and are completely absent from acinar cells. In humans, they are present in approximately 23% of beta cells and in <5% of alpha-, delta-, and PP cells combined [2]. The physiological significance of beta cell INRs is presently unknown; however, preliminary studies in our laboratory indicate that these are highly dynamic nuclear bodies rather than static protein aggregates.

The molecular mechanisms underlying beta cell INR formation are currently unknown. As an approach to identifying the possible molecular mediators of INR formation in beta cells, we examined INRs in mice with a conditional beta cell-specific knockout of serine/threonine kinase Lkb1 (Lkb1 adult beta cell knockout, LABKO mice) [4]. As a broad-spectrum regulator of beta cell function [5], Lkb1 is an attractive initial candidate for this approach as it regulates many aspects of beta cell structure and function. It achieves this via phosphorylation and consequent activation of members of the 5′ AMP-activated protein kinase (AMPK) family [6]. Accordingly,

the beta cells of LABKO mice are larger due to the loss of AMPK-mediated suppression of the mammalian target of rapamycin (mTOR) and display what appears to be abnormal cell polarity due to the loss of microtubule affinity-regulating kinase 2 (Mark 2) activity [4, 7]. Functionally, LABKO animals display enhanced basal and nutrient-stimulated insulin secretion and are resistant to high-fat diet (HFD)-induced impairment of glucose tolerance [4, 7].

In the present study, we first compared the frequency of beta cell INRs in LABKO and control mice maintained on either normal (chow) diet or a HFD, an extensively used model of human metabolic syndrome and an inducer of diabetic transformation in mice [8]. To probe further the status of beta cell INRs in a pathological context, we investigated them in an unrelated mouse model of T2D which has been widely used as a model of the human prediabetic state, the leptin-deficient ob/ob mouse [9].

Materials and Methods.

Mice.

LABKO Mice. Pancreatic tissues from LABKO and control mice reported in the previous study of Fu et al. [4] were employed in the present study. Generation and characterization of LABKO mice, including the absence of Lkb1 in LABKO islets as well as the morphometric analysis of islet and beta cell size, was previously described [4]. Briefly, $Lkb1^{loxP/loxP}$ (L/L; FVB/n background) [10] and Pdx-CreERt2 mice (ICR background; kind gift of D. Melton) were mated to generate $Lkb1^{loxP/loxP}$, Pdx-CreERt2 (LABKO) mice. The Pdx-CreERt2 mice were backcrossed three times onto FVB/n background and then were intercrossed. To induce Lkb1 gene ablation, 5 mg of tamoxifen (Sigma) per 40 g of body weight mass was injected intraperitoneally every second day for a total of three injections. LABKO and L/L control mice were 10–12 weeks old at the time of killing and showed no significant difference in their mean body weight (27 ± 0.7 vs. 28 ± 0.8, respectively, p=0.36) or the wet weight of extracted pancreata (0.296 ± 0.017 vs. 0.246 ± 0.060 respectively, p=0.12).

Mark2 Knockout Mice. Tissues from 12- to 14-week-old Mark 2/EMK+/− mice were a kind gift from H. Piwnica-Worms. The generation of these mice and their characterization has been described previously [11].

ob/ob Mice Leptin-null, male, 11-week-old ob/ob mice and their wild type C57/B6 littermate controls were purchased from Jackson Labs. The ob/ob mice were visibly obese and had significantly elevated fasted blood glucose levels (10.9±0.8mM compared to 6.6±0.5mM in controls, $p<0.003$). Mice were killed at 12 weeks of age following an overnight fast.

Treatments.

For HFD studies, mice were fed normal laboratory chow diet or 45% of total caloric intake derived from fat (HFD; Open Source Diets) for 16 weeks. Body weights of LABKO (34.8 ± 2.5 g) and L/L (35.1 ± 2.3 g) mice were not significantly different from one another ($p=0.91$). However, they were significantly higher than their respective counterparts on a normal chow diet ($p=0.00005$ for LABKO and $p=0.02$ for L/L). Rapamycin (0.6 mg/kg; LC Laboratories) was injected every second day for a total of three injections starting 1 day after the last tamoxifen injection. All procedures involving mice were approved by the Animal Care Committee of the University of Ottawa.

Immunostaining and Image Analysis.

Pancreata from LABKO and their L/L controls were isolated after perfusion with 4% paraformaldehyde in PBS, weighed, and stored in fixative overnight at RT. Pancreata from ob/ob and their C57/B6 controls were immersion-fixed in 10% neutral-buffered formalin for 1 week at RT. Tissues were embedded in paraffin and 4-μm sections prepared. For the detection of INRs and beta cells, sections were stained with a mixture of anti-C3T (mouse monoclonal SDL.3D10, 1:100, Sigma, St Louis, MO, USA) and an antibody to insulin (rabbit polyclonal H-86, 1:600; Santa Cruz Biotechnologies, Santa Cruz, CA, USA). Secondary antibodies for immunofluorescence detection were as follows: AlexaFluor 488 goat anti-mouse IgG (H+L) and AlexaFluor 594 donkey anti-rabbit IgG (H+L) (Molecular Probes). Sections were mounted using Vectashield mounting medium with DAPI as a nuclear counterstain and examined using a Zeiss Axioplan II fluorescence microscope (Carl Zeiss Microscopy, Germany) with attached AxioCam

digital camera. For each mouse, images of pancreatic islets (10–50 per mouse) were acquired using three-color multidimensional acquisition. Blinded, manual counts of beta cell nuclei and INR containing beta cell nuclei were performed. Data were analyzed by ANOVA using SigmaStat (Systat Software, Inc.) statistical software and presented as mean INR frequency ± SEM.

Results.

Appearance of INRs in Mouse Islets is Similar to Human Islets.

INRs were present in beta cell nuclei of all mice examined (Fig. 1). Consistent with our observations in human islets [2], INRs were predominantly rod-shaped (Fig. 1b, arrow). In some cells, they appeared as single, intensely stained dots (Fig. 1b, arrowhead). In these instances, gradual transition through the z-plane of the optical section resulted in a continuous, uninterrupted shift in the position of the dot in the XY plane, as would be expected for rods oriented at an oblique angle with respect to the plane of the optical section. Also consistent with our human studies, INRs were rarely observed within the nuclei of insulin-negative islet cells and never in acinar cells.

Beta Cell INR Frequency is Reduced in LABKO Mice.

In order to examine the potential effects of Lkb1 on INR formation, beta cell INR frequency was compared in the islets of LABKO and control (L/L) mice. As shown in Fig. 2, beta cell INR frequency was reduced by more than twofold in LABKO mice compared to L/L controls under both normal diet (14.3 ± 4.6% vs. 35.8 ± 1.6%, respectively, $p<0.005$, n=3) and HFD conditions (2.8±0.2% vs. 21.3±1.7%, respectively, $p<0.01$, n=3).

Beta Cell INR Depletion in LABKO Mice Is Not Mediated By the Lkb1 Effectors mTOR or Mark2.

Loss of inhibition of mTOR and loss of activation of Mark2 have been previously reported as key downstream effectors of the Lkb1-null beta cell phenotype [4, 7]. Injections of

Figure 1.

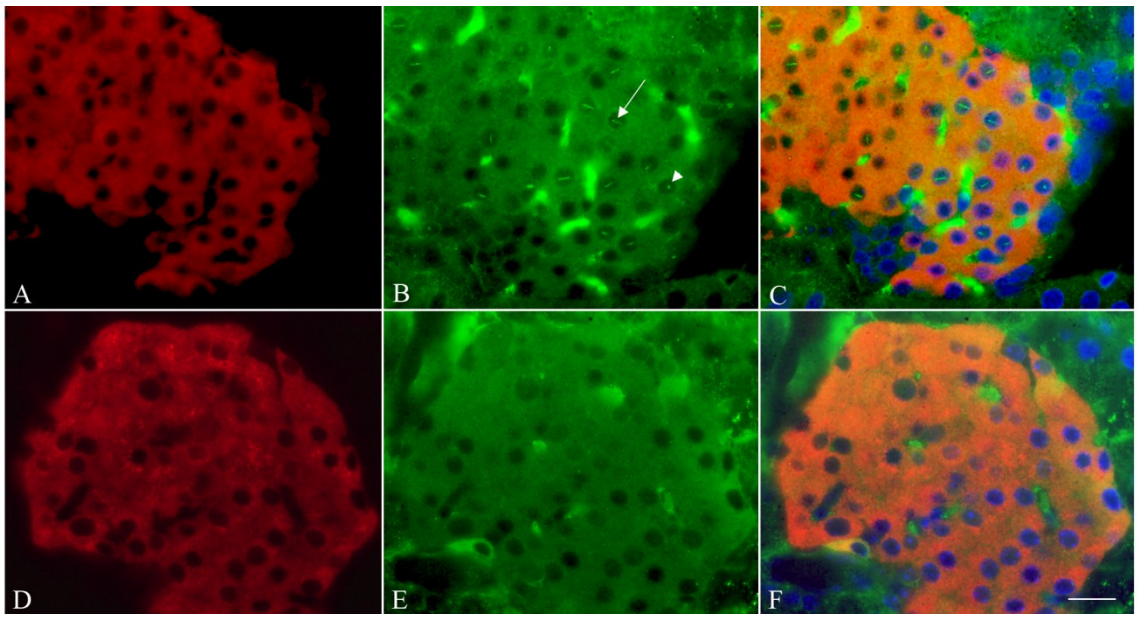

Legend to Figure 1.

Islets of Langerhans in L/L (a–c) and LABKO (d–f) mice double-immunostained for insulin (red) (a, d) and C3T (green) (b, e). Merged images shown with DAPI nuclear counterstain (blue) in c, f. In L/L mice, multiple INRs are visible in beta cells as rod-shaped intranuclear structures (arrow in b) or as dot-shaped profiles viewed "end-on" (arrowhead in b). No INRs are visible in the LABKO islet. Bar in F=20 μM

Figure 2.

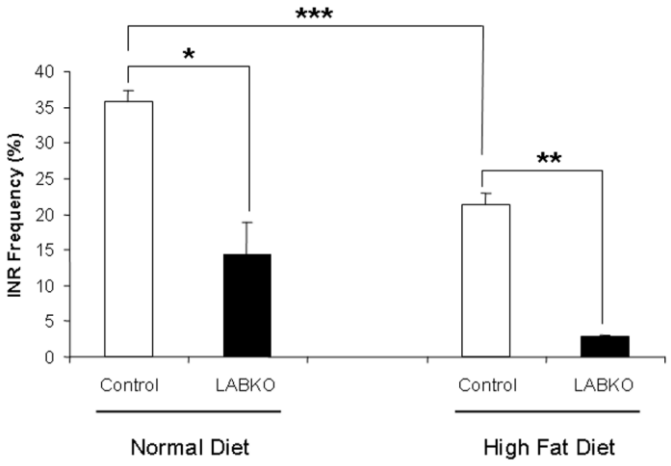
***
*
**
INR Frequency (%)
40
35
30
25
20
15
10
5
0
Control
LABKO
Control
LABKO
Normal Diet
High Fat Diet

Legend to Figure 2.

The proportion of beta cells containing INRs (INR frequency) is significantly reduced in LABKO vs. L/L (control) mice under both ND (*$p<0.05$) and HFD (**$p<0.01$) conditions. In L/L (control) mice, those maintained on a HFD show significantly reduced INR frequency vs. those on a ND (***$p<0.005$). Data shown are mean ±SEM; n=3 in each group.

the mTOR inhibitor rapamycin were previously shown to reverse the beta cell hypertrophy phenotype of LABKO mice [4]. Treatment with rapamycin resulted in a further reduction in beta cell INRs (15.4 ± 8.4% vehicle vs. 5.4 ± 2.8% rapamycin, $p<0.05$, n=4; Fig. 3a); thus, the decrease in INRs in LABKO mice does not involve cell size or increased mTOR activity.

To determine whether the loss of activation of Mark2 was responsible for INR depletion in LABKO mice, INRs were examined in Mark2 knockout mice and their respective controls. As shown in Fig. 3b, Mark2 knockout mice exhibited no alterations in the proportion of INR-containing beta cells (11.8±3.3% Mark2+/+, 8.7±2.8% Mark2+/−, 11.3±3.9% Mark2−/−).

Beta Cell INRs are Depleted in Normal Mice Maintained on a HFD.

L/L control mice were maintained on either a normal diet or a HFD for a period of 16 weeks. As expected, HFD mice developed features reminiscent of human metabolic syndrome, as has been described in detail previously [4]. They displayed a >40% reduction in INR content compared to normal diet group (21.3±1.7% vs. 35.8±1.6%, $p<0.005$, n=3; Fig. 2).

Beta Cell INRs are Dramatically Reduced in ob/ob Mice.

The reduction of beta cell INR frequency associated with HFD-induced metabolic syndrome prompted us to investigate beta cell INR prevalence in another mouse model of diabetes, the leptin-deficient ob/ob mouse. As shown in Fig. 4a, the islets of 12-week-old hyperglycemic, obese ob/ob mice exhibited a dramatic depletion of beta cell INRs relative to controls (Fig. 4a). Quantitative analysis (Fig. 4b) revealed a 19-fold reduction (32.6±2.5% vs. 1.7±0.4%, respectively, $p<0.001$, n=4).

Figure 3.

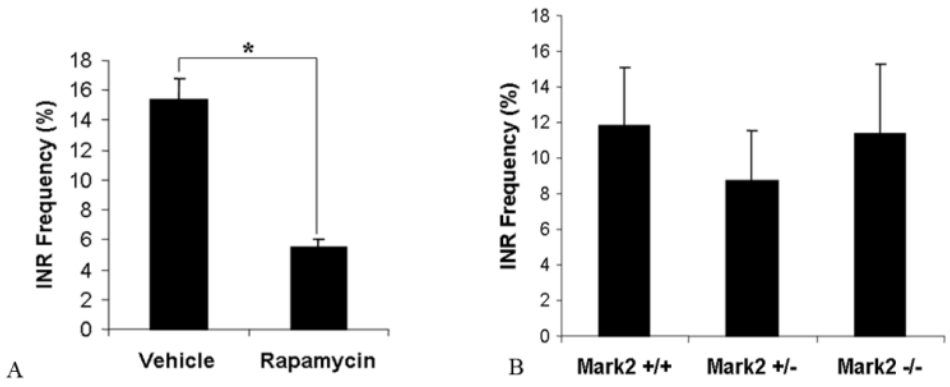
INR Frequency (%)
18
16
14
12
10
8
6
4
2
0
*
Vehicle
Rapamycin
A
INR Frequency (%)
18
16
14
12
10
8
6
4
2
0
Mark2 +/+
Mark2 +/-
Mark2 -/-
B

Legend to Figure 3.

A The proportion of beta cells containing INRs (INR frequency) is reduced in LABKO (*$p<0.05$) mice treated with rapamycin. Data shown are mean ± SEM; n=3 in each group.

B The proportion of beta cells containing INRs (INR frequency) is not significantly different among Mark2 control (Mark2+/+), heterozygous (Mark2+/−), and homozygous (Mark2−/−) Mark2 knockout mice. Data shown are mean ± SEM; n=4 in each group.

Figure 4.

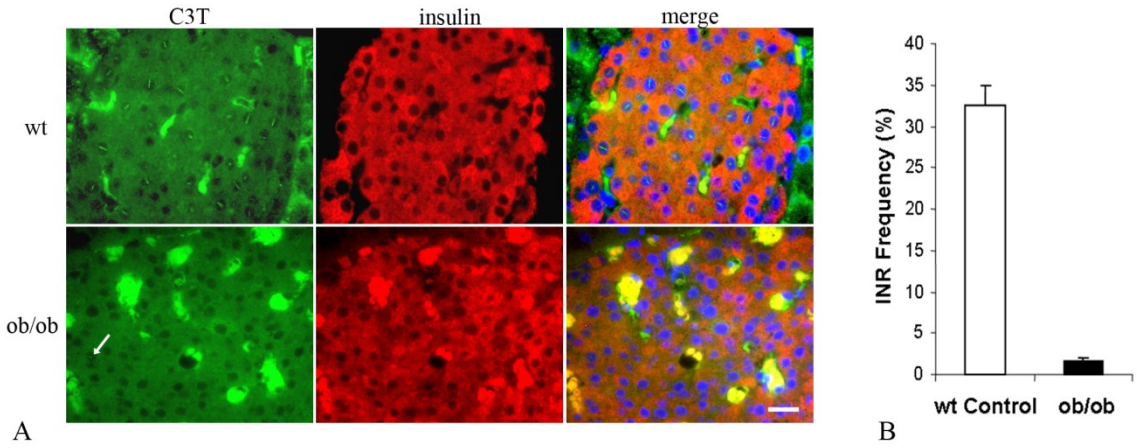
C3T
insulin
merge
wt
ob/ob
A
INR Frequency (%)
40
35
30
25
20
15
10
5
0
wt Control
ob/ob
B

Legend to Figure 4.

A Islets of Langerhans in wild-type (wt, top row) and ob/ob (bottom row) mice double-immunostained for insulin (red) and C3T (green). Merged images shown with DAPI nuclear counterstain (blue). In wild-type mice, multiple INRs are visible in beta cells as rodshaped intranuclear structures. Only a single INR (arrow) is seen in the ob/ob islet. Bar, 30 μM.

B Quantitative analysis reveals a marked reduction in INR frequency in ob/ob mice compared to wild-type controls ($p<0.001$). Data shown are mean ± SEM; n=4 in each group

Discussion

INRs are a prominent yet poorly understood morphological feature of pancreatic beta cell nuclei. This study extends our previous demonstration of INRs in human pancreatic islet cells [2], confirming their presence in mouse beta cells. Moreover, we demonstrate that the presence of INRs in beta cells is regulated, and we provide evidence that beta cell INRs may be of pathophysiological relevance to diabetes. These new observations will provide a framework for a detailed analysis of INR dynamics using additional mouse models of diabetes with varying beta cell function imposed by genetic or pharmacological manipulation.

In search of molecular regulators of INR formation, we demonstrated a significant loss of INRs in LABKO mice relative to controls under both normal diet and HFD conditions. This suggested that INR formation in beta cells might be regulated by Lkb1 or by one or more of its downstream effectors in the AMPK family [6]. However, INR depletion in LABKO beta cells was not mediated by the two key Lkb1 effectors, mTOR or Mark2. It is noteworthy that the Lkb1-induced suppression of microtubule polymerization is mediated through the activation of Mark2. Thus, although INRs are immunoreactive for the beta-tubulin subtype C3T, their depletion in LABKO mice does not appear to be related to the Lkb1-mediated regulation of microtubule polymerization [12]. Furthermore, although INR depletion is characteristic of LABKO, ob/ob, and HFD mice, the latter two models actually have elevated levels of beta cell Lkb1 [4]. This suggests that the immediate effector of INR depletion does not lie directly within the Lkb1 signalling pathway but instead that INR changes in LABKO mice are an indirect consequence of the functional alterations induced in beta cells by Lkb1 depletion. Thus, it is possible that INR depletion in LABKO mice results from some feature common to all three

models examined here. Potential candidates currently being tested include enhanced beta cell insulin production or secretion, islet neogenesis, or islet hyperplasia [4, 7].

We have previously reported a dramatic loss of INRs in human postmortem brain samples derived from Alzheimer's disease patients relative to age-matched controls [13]. Here, we extend the potential pathological relevance of INRs to diabetes by demonstrating a significant reduction in beta cell INRs in the HFD-induced disease paradigm and even more dramatically in the leptin-deficient ob/ob mouse model of diabetes. Both the HFD and the ob/ob mice are models of obesity-related insulin resistance and hyperglycemia. It is possible that underlying metabolic changes of pathophysiological relevance are the modulators of INR frequency in ob/ob and HFD mice. In this context, it will be interesting to determine whether INR depletion can be reversed in these models by exogenous leptin administration or reversion to a normal diet, respectively. In addition, it will be important to examine the effects of clinically relevant therapeutics on beta cell INRs in these models.

The results of the present study represent the first report of the regulation of INR frequency in pancreatic beta cells. In light of considerable evidence for beta cell dysfunction in the pathogenesis of T2D [14], our results introduce INRs as a new marker of beta cell function with the potential to further our understanding of beta cell biology in both normal and diabetic conditions.

Acknowledgments. This study was supported by The Physicians Services Incorporated Foundation 09-01 awarded to JMW and by a CIHR grant to RAS (MOP: 84244). RAS holds the Canada Research Chair in Apoptotic Signaling.

References

1. Wajchenberg BL: Beta-cell failure in diabetes and preservation by clinical treatment. *Endocr Rev* 28:187–218, 2007

2. Prichett W, Milman P, Gagnon J, Munoz DG, Woulfe J: Intranuclear rodlets in human pancreatic islet cells. *Pancreas* 35:207–211, 2007

3. Woulfe J, Munoz D: Tubulin immunoreactive neuronal Intranuclear inclusions in the human brain. *Neuropathol Appl Neurobiol* 26:161–171, 2000

4. Fu A, Ng AC, Depatie C, Wijesekara N, He Y, Wang GS, Bardeesy N, Scott FW, Touyz RM, Wheeler MB, Screaton RA: Loss of Lkb1 in adult beta cells increases beta cell mass and enhances glucose tolerance in mice. *Cell Metab* 10:285–295, 2009

5. Bright NJ, Thornton C, Carling D: The regulation and function of mammalian AMPK-related kinases. *Acta Physiol (Oxf)* 196:15–26, 2009

6. Lizcano JM, Goransson O, Toth R, Deak M, Morrice NA, Boudeau J, Hawley SA, Udd L, Makela TP, Hardie DG, Alessi DR: LKB1 is a master kinase that activates 13 kinases of the AMPK subfamily, including MARK/PAR-1. *EMBO J* 23:833–843, 2004

7. Granot Z, Swisa A, Magenheim J, Stolovich-Rain M, Fujimoto W, Manduchi E, Miki T, Lennerz JK, Stoeckert CJ, Jr., Meyuhas O, Seino S, Permutt MA, Piwnica-Worms H, Bardeesy N, Dor Y: LKB1 regulates pancreatic beta cell size, polarity, and function. *Cell Metab* 10:296–308, 2009

8. Islam MS, Loots du T: Experimental rodent models of type 2 diabetes: a review. *Methods Find Exp Clin Pharmacol* 31:249–261, 2009

9. Lindstrom P: The physiology of obese-hyperglycemic mice [ob/ob mice]. *ScientificWorldJournal* 7:666–685, 2007

10. Hezel AF, Gurumurthy S, Granot Z, Swisa A, Chu GC, Bailey G, Dor Y, Bardeesy N, Depinho RA: Pancreatic LKB1 deletion leads to acinar polarity defects and cystic neoplasms. *Mol Cell Biol* 28:2414–2425, 2008

11. Hurov JB, Huang M, White LS, Lennerz J, Choi CS, Cho YR, Kim HJ, Prior JL, Piwnica-Worms D, Cantley LC, Kim JK, Shulman GI, Piwnica-Worms H: Loss of the Par-1b/MARK2 polarity kinase leads to increased metabolic rate, decreased adiposity, and insulin hypersensitivity in vivo. *Proc Natl Acad Sci U S A* 104:5680–5685, 2007

12. Kojima Y, Miyoshi H, Clevers HC, Oshima M, Aoki M, Taketo MM: Suppression of tubulin polymerization by the LKB1-microtubule-associated protein/microtubule affinity-regulating kinase signaling. *J Biol Chem* 282:23532–23540, 2007

13. Woulfe JM, Hammond R, Richardson B, Sooriabalan D, Parks W, Rippstein P, Munoz DG: Reduction of neuronal Intranuclear rodlets immunoreactive for tubulin and glucocorticoid receptor in Alzheimer's disease. *Brain Pathol* 12:300–307, 2002

14. Muoio DM, Newgard CB: Mechanisms of disease: molecular and metabolic mechanisms of insulin resistance and beta-cell failure in type 2 diabetes. *Nat Rev Mol Cell Biol* 9:193–205, 2008

Chapter 3.

The manuscript contained in this chapter had been submitted for publication in the *Journal of Comparative Neurology*. It has been reviewed and is undergoing the revisions recommended by the referees and editors prior to resubmission.

Statement of student's contribution:
Data collection and analysis was performed by Pavel Milman. Pavel also was the principal writer of the manuscript. The manuscript was jointly edited by Dr. Woulfe and Pavel Milman.

John Woulfe,

Pavel Milman.

Foreword:

Biochemical heterogeneity of INRs is a relatively new concept of potentially great significance for our understanding of their biological function and for the way we approach INR research. In support of this new concept, I have discovered a new INR subtype immunoreactive for Hap40 and distinct from SDL-INRs, which we have previously observed in mouse brain. This chapter describes the characterization of Hap40-INRs in the mouse brain, their relation to SDL-INRs and the evidence for the existence of another potential new subtype of INR currently defined by its exclusive immunoreactivity for ubiquitin.

A Novel Variant of Neuronal Intranuclear Rodlet Immunoreactive for 40 kDa Huntingtin Associated Protein and Ubiquitin in the Mouse Brain.

Pavel Milman[1, 3], John Woulfe[1, 2, 3]

[1]-Department of Biochemistry, Microbiology and Immunology, University of Ottawa

[2]-Department of Pathology and Laboratory Medicine, University of Ottawa

[3]-Centre for Cancer Therapeutics, Ottawa Hospital Research Institute

Abbreviated Title: Hap40 INRs in mouse brain.

Name of Associate Editor to whom the manuscript is being submitted: Paul E. Sawchenko

Key words: rodlet of Roncoroni, hypothalamus, locus coeruleus, nuclear bodies, melanin concentrating hormone

Corresponding author:

Dr. John Woulfe

Dept. of Pathology, The Ottawa Hospital, Civic Campus

Funding for this study was provided by the Physicians Services Incorporated Foundation Inc.

Abstract.

Intranuclear rodlets (INRs), also known as rodlets of Roncoroni, are poorly understood intranuclear bodies originally identified within neuronal nuclei on the basis of their unique morphology. The mechanisms of their formation, their biochemical composition and their physiological significance remain unknown. Using double immunofluorescence staining of mouse brain sections, we have identified a novel variant of INR that is immunoreactive for the 40kDa huntingtin associated protein (Hap40) and ubiquitin, and provided evidence for the existence of additional INR subtypes sharing ubiquitin immunoreactivity as a common feature. We describe a selective association of these INRs with melanin concentrating hormone (MCH) and tyrosine hydroxylase immunoreactive neurons of the hypothalamus and the locus coeruleus, respectively. We also demonstrate for the first time that biochemically distinct INR subtypes can co-exist within a single nucleus where they engage in non-random spatial interactions. Our findings highlight the biochemical diversity and cell type specific expression of these enigmatic intranuclear structures.

Introduction.

There is growing appreciation for the concept of compartmentalization of nuclear functions into discrete spatial domains or "nuclear bodies" (Spector, 1993). Some of the classical examples include nucleoli, Cajal (coiled) bodies, promyelocytic leukemia (PML) bodies, nuclear speckles, Gemini of coiled bodies (Gems), among others. Whereas specific functional roles have been ascribed to some nuclear bodies, functional niches for others remain enigmatic. Although the majority of these nuclear bodies are ubiquitous, some are confined to specific cell types. The intranuclear rodlet (INR), also known as the rodlet of Roncoroni (Roncoroni, 1895) is one such structure found predominantly in the nuclei of neurons (Cajal, 1909; Masurovsky et al., 1970; Woulfe and Munoz, 2000) and pancreatic beta-cells (Milman et al., 2010; Prichett et al., 2007). It is a prominent rod or bar shaped nuclear body that was first described more than a century ago by early microscopists, including Santiago Ramon Y Cajal (Cajal, 1909), in certain neuronal populations using classical histological staining techniques (Marinesco, 1902; Roncoroni, 1895). With the advent of electron microscopy, a number of reports emerged in the 1960's through the 1980's describing the ultrastructural features of neuronal INRs within the nervous system of a variety of vertebrate as well as non-vertebrate species (Gray and Guillery, 1963). A few of these ultrastructural studies attempted to address the physiological significance of INRs. Notably, Seite and co-workers demonstrated that INRs in cat sympathetic ganglia were dynamic structures whose formation could be induced by electrical stimulation (Seite et al., 1971) and by the intracellular second messenger cAMP (Seite et al., 1977). More recent studies have confirmed the dynamic nature of INRs and suggested a link between their formation and transcriptional/translational activity (Villagra et al., 2008). Despite these efforts, the

physiological significance, biochemical composition, and mechanism of formation of neuronal INRs remain largely unknown. In 2000, we described the presence of rod-shaped intranuclear structures within neurons of the non-diseased human brain using a commercially available monoclonal antibody SDL.3D10 directed against the neuron specific cytoskeletal protein class III beta tubulin (Woulfe and Munoz, 2000). Ultrastructurally, these structures displayed features identical to those described for INRs. These SDL.3D10 immunoreactive INRs (heretofore referred to as "SDL-INRs") were also found to be immunoreactive using a polyclonal antibody (GR P-20) against glucocorticoid receptor (Woulfe et al., 2002). The ability to detect INRs immunohistochemically provided a novel contemporary tool to investigate their distribution and physiological relevance. In the human brain, SDL-INRs displayed a widespread, stereotyped topographic pattern of distribution (Woulfe and Munoz, 2000). Remarkably, they were markedly reduced in the temporal cortex of patients with Alzheimer's disease relative to age matched controls and patients with a closely related neurodegenerative disease, dementia with Lewy bodies (Woulfe et al., 2002), suggesting that they may have pathophysiological relevance. The prevalence of SDL-INRs was also altered in dopaminergic neurons in substantia nigra of the MPTP-induced mouse model of Parkinson's disease (Lamba et al., 2005). In the human substantia nigra, INRs exhibit unique features not seen in other brain areas. Specifically, a large proportion of nigral INRs are surrounded by a shell of intense immunostaining for promyelocytic leukemia (PML) protein, the signature constituent protein of PML nuclear bodies. A subset of these were also immunoreactive for ubiquitin, proteasome subunits, and small ubiquitin modifier 1 (SUMO1) as well as transcriptionally relevant proteins including cAMP response element binding protein (CBP) and acetylated histone H4 (Woulfe et al., 2004; Woulfe et al., 2007). The existence of these INR variants suggests that INRs in different neuronal populations may be heterogeneous in terms of their biochemical composition and, perhaps, function. Consistent with

this possibility, Berciano et al. reported an immunologically distinct type of INR in the rat supraoptic nucleus (SON). It did not stain for SDL.3D10 but was intensely positive for poly(A) binding protein nuclear 1 (PABPN1), the disease protein of oculopharyngeal muscular dystrophy. This subtype of INR (PABPN-INR) also labelled for polyadenylated RNA, the 19S regulatory and 20S catalytic subunits of the proteasome, and ubiquitin. Notably, the authors demonstrated that PABPN- and SDL-INRs localized to neurochemically distinct neuronal subpopulations within the SON (Berciano et al., 2004). We therefore took advantage of immunological staining methods to further extend the notion of INRs as a biochemically diverse family of nuclear bodies with INR subtype-specific patterns of distribution among specific neurochemically and/or anatomically defined neuronal populations.

Materials and methods.

Animal models.

Animal procedures were approved by the Ottawa Hospital Research Institute Animal Care Committee, in accordance with the Canadian Council on Animal Care guidelines. CD-1 wild type mice (Charles River, Canada) were housed for at least one week before euthanasia. Brain tissue was extracted and processed for western blotting or immunofluorescence microscopy as described below.

Protein extraction and Western blotting.

HeLa cell lysate was obtained from Transduction Laboratories. Total brain protein was extracted with either reducing SDS containing(125 mM Tris-HCl buffer pH6.8, 2% SDS, 5% β-mercaptoethanol, and 10% glycerol) or non-reducing Triton X-100 containing (50 mM Tris-HCl buffer pH7.6, 1% Tritin X-100, 150 mM NaCl, 1 mM EDTA) extraction buffer, supplemented with Complete Mini protease inhibitor cocktail (Roche Applied Science). Brain extracts were cleared by centrifugation at 18 000g for 10 min. 20 μg of HeLa cell protein or 30 μg of mouse brain protein were separated by SDS-PAGE, transferred onto PVDF (0.45 μm Immobilon-P, Millipore) membrane and probed with anti-Hap40 antibody ab5872 (1:1000; Chemicon/Millipore) or RA19010 (1:2000; Neuromics). Hap40 immunoreactive bands were detected using horseradish peroxidase-conjugated anti-rabbit IgG secondary antibodies (1:5000; NA9340, Amersham). As a loading control, membranes were stripped of antibodies using Re-

Blot Plus Strong solution (#2504; Millipore) in accordance with manufacturer's instructions and re-probed with anti-actin monoclonal antibody (1:500; clone C4, Millipore).

Tissue preparation and immunofluorescence.

CD-1 wild type mouse brains were immersion fixed in 10% neutral buffered formalin for 1 week at RT. Tissues were embedded in paraffin and 4 μm sections prepared. Sections were deparaffinized in toluene and re-hydrated in a series of graded alcohols. Where indicated (see Table 1), tissue was subjected to antigen retrieval (AR) by microwaving for 10 min. in 600 ml of TE (10 mM Tris; 1 mM EDTA; pH9) buffer prior to immuno-fluorescence staining. Secondary antibodies for immunoflurescence detection were as follows: AlexaFluor 488 goat anti-mouse IgG (H+L); AlexaFluor 594 donkey anti-rabbit IgG (H+L) and AlexaFluor 488 chicken anti-goat IgG (H+L) (Invitrogen, Molecular Probes). Sections were mounted using Vectashield mounting medium with DAPI as a fluorescent nuclear counterstain and examined using a Zeiss Axioplan II fluorescence microscope (Carl Zeiss Microscopy, Germany) mounted with an AxioCam digital camera.

Antibody characterization.

Please see Table 1 for a list of all primary antibodies used.

Detection of Hap40 protein in western blotting and immunofluorescence experiments using anti-Hap40 antibody ab5872 has been previously described (Pal et al., 2006). The authors performed western blots on bovine brain protein isolated on a column with immobilized Rab5-

Table 1. Antibodies used in this study.

Target Protein	Name/ Cat#	Source	Immunogen	Dilution	Host species	Antigen retrieval
Actin	Clone C4	Millipore	Purified chicken gizzard actin	1:500	mouse	N/A
Class III β-tubulin	SDL.3D10	Sigma	Synthetic peptide CESESEQGPK	1:200	mouse	No
Hap1	sc-30126	SantaCruz	Recombinant protein with a.a. 329-628 of mouse HAP1b	1:50*	rabbit	**
Hap40	ab5872	Chemicon/ Millipore	Synthetic peptide corresponding to a.a. 314-326 of mouse Hap40	1:100	rabbit	No
Hap40	RA19010	Neuromics	Synthetic peptide corresponding to a.a. 314-326 of mouse Hap40	1:100	rabbit	No
Huntingtin	MAB2166	Chemicon/ Millipore	Recombinant protein with a.a. 181-810 of human huntingtin	1:50*	mouse	**
pro-MCH	sc-14509	SantaCruz	a.a. 115-165*** near C-terminal of human proMCH	1:200	goat	Yes
NPY	3F11	Abnova	Recombinant GST-tagged protein with a.a. 29-97 of human NPY	1:50*	mouse	Yes
Orexin	sc-8071	SantaCruz	Synthetic peptide corresponding to a.a. 78-96 of human orexin B	1:200	goat	Yes
PML	MAB3738	Chemicon/ Millipore	Recombinant His-tagged protein with a.a. 1-581 of mouse PML	1:50*	mouse	**
PML	sc-9862	SantaCruz	a.a. 10-60*** near N-terminus of human PML	1:50*	goat	**
POMC	ab73092	Abcam	Synthetic peptide corresponding to a.a. 1-24 of human POMC	1:200	mouse	Yes
Rpt5, 19S proteasome	TBP1-19	BioMol/ Millipore	Full length human recombinant Rpt5 protein.	1:50*	mouse	**
Tyrosine Hydroxylase	MAB318	Chemicon/ Millipore	Tyrosine hydroxylase purified from PC12 cells	1:200	mouse	Yes
Ubiquitin	Ub-Fl76 (sc-9133)	SantaCruz	Recombinant protein with a.a. 1-76, full length human ubiquitin	1:200	rabbit	Yes/No
Ubiquitin	Ubi-1	Abcam	Keyhole limpet hemocyanin-conjugated full length ubiquitin	1:100	rabbit	Yes/No

* - Lowest tested antibody dilution is indicated. ** - Tested with and without antigen retrieval. *** - Indicated is a 50 amino acid range for the synthetic peptide immunogen sequence (Santa Cruz, personal comunication). No - Without antigen retrieval. Yes - With antigen retrieval. Yes/No - With or without antigen retrieval.

GST preloaded with either GDP or non-hydrolysable GTP analog GTγP. Consistent with specific Hap40 interaction with GTP bound Rab5, the figure shows a doublet immunoreactive against Hap40 antibody ab5872 in the eluate from GTγP but not GDP preloaded Rab5-GST column. Although the position of molecular weight markers was not indicated in the figure, the authors estimated the molecular weight of the major band at 40kDa. Our own western blotting analysis of mouse brain protein extracts using the same anti-Hap40 antibody ab5872 revealed a similar doublet; however, our molecular weight estimates put it at ~30kDa. We also performed side by side western blotting and immunofluorescence experiments using ab5872 and another anti-Hap40 antibody, RA19010 (Neuromics). The results produced using ab5872 and RA19010 anti-Hap40 antibodies were indistinguishable from each other.

Generation and characterization of a monoclonal anti-actin antibody clone C4 was first described by Lessard J.L. and was reported to cross-react with all six vertebrate actin isoforms (Lessard, 1988).

Generation and characterization of the SDL.3D10 monoclonal antibody against class III beta tubulin was first described by (Banerjee et al., 1990). Its use for detection of neuronal INRs has been previously described (Woulfe and Munoz, 2000). Immunostaining of INRs was eliminated by pre-incubation of the antibody with a synthetic peptide corresponding to the immunogenic peptide used to create the antibody.

The anti-Hap1 rabbit polyclonal antibody sc-30126 (M-300) produced granular cytoplasmic, mostly perinuclear staining pattern in neurons throughout mouse brain. Importantly, this antibody detected large (~up to 3µm in diameter) perinuclear bodies with donut-shaped appearance characteristic of Hap1 immunoreactive stigmoid bodies described on light and electron microscopic levels by Gutenkunst et al. (Gutekunst et al., 1998). In the mouse brain, these structures were found most often in the lateral septum but were also present in other brain

regions.

The anti-Huntingtin monoclonal MAB2166 antibody detected huntingtin in western blots of Hap40 immunoprecipitated mouse brain protein (Peters and Ross, 2001). Immunofluorescence signal from MAB2166 antibody in mouse brain sections was reduced 50 to 75% following Huntingtin knock down by in utero transfection of Huntingtin-specific shRNA (Tong et al., 2011).

Specificity of the anti-proMCH antibody (sc-14509, Santa Cruz) has been previously determined by double staining immunofluorescence experiments with another anti-MCH antibody (H-070-47; Phoenix Pharmaceuticals).The latter was raised against the full length 19 amino acid MCH peptide and its specificity was determined by competition radioimmunoassay by the manufacturer (Deurveilher et al., 2006). In addition, the authors reported a virtually complete co-localization of the two antibodies to the same neurons of the hypothalamus and zona incerta. This staining was abrogated by preincubation of the anti-MCH antibody with immunogenic peptide (Deurveilher et al., 2006).

The anti-orexin B antibody (sc-8071, Santa Cruz) was raised against a synthetic peptide corresponding to amino acids 78-96 of human orexin-B (Bullmann et al.). Its specificity was previously confirmed by double staining immunofluorescence experiments with either a rabbit polyclonal anti-orexin B antibody (H-003-32; Phoenix Pharmaceuticals; specificity determined by competition radioimmunoassay by the manufacturer) or a rabbit polyclonal anti-preproorexin antibody (AB3096; Chemicon) raised against a synthetic peptide corresponding to the last 17 amino acids of mouse preproorexin precursor protein. Double-immunofluorescence staining using the Santa Cruz anti-orexin B antibody and either of the other two aforementioned anti-orexin B antibodies was reported to show virtually complete overlap of cell body staining (Deurveilher et al., 2006).

Both MCH and orexin antibodies produced intense cytoplasmic staining in neurons of the lateral hypothalamic area located primarily around and dorso-lateral to the fornix. In addition, MCH -positive cell bodies were frequently observed in the zona incerta where few, if any, orexin positive neurons have been observed. MCH positive neurons were also more numerous than orexin positive neurons in the more caudal sections of hypothalamus that displayed a prominent subthalamic nucleus at this level. These observations are consistent with previously reported distribution of MCH and orexin neurons (Broberger et al., 1998).

The mouse monoclonal anti-tyrosine hydroxylase antibody (MAB318, Chemicon) was raised against tyrosine hydroxylase (TH) purified from PC12 cells. It recognizes an epitope on the outside of the regulatory N-terminus of TH. On Western blot it detects a protein of approximately 59–63 kDa and does not cross-react with dopamine-beta-hydroxylase, phenylalanine hydroxylase, trytophan hydroxylase, dehydropteridine reductase, sepiapterin reductase or phenethanolamine-N-methyl transferase (as reported by the manufacturer). We have detected intensely tyrosine hydroxylase-immunoreactive cell bodies in substantia nigra pars compacta and in the locus coeruleus.

The anti-POMC antibodies stained neuronal cell bodies in the arcuate nucleus and occasionally in the medial hypothalamus in the vicinity of the fourth ventricle consistent with the established anatomical distribution of POMC and its derivative peptide hormones expressing neurons in the hypothalamus.

The anti-NPY antibody detects GST-tagged, partial recombinant NPY protein on western blot (as reported by manufacturer). Immunofluorescence analysis produced a characteristic staining pattern of neuronal projections in the posterior hypothalamus including projections to the paraventricular nucleus and the arcuate nucleus were the NPY positive neuronal cell bodies were expected. However, in the absence of cholchicine pre-treatment, the antibody failed to reliably

identify neuronal cell bodies in the arcuate nucleus of hypothalamus.

The use of the goat polyclonal anti-PML N-19 antibody for the detection of PML bodies and PML immunoreactive INRs has been previously described (Woulfe et al., 2007). We have also detected typical PML nuclear bodies using MAB3738 monoclonal antibody.

Detection of the 19S proteasomal subunit in INRs by the anti-Rpt5 monoclonal antibody TBP1-19 has been previously described (Berciano et al., 2004). We observed predominantly diffused nuclear staining. Occasionally this antibody detected small nuclear granules that were also ubiquitin immunoreactive and likely represent clastosomes, nuclear sites of proteasome mediated protein degradation.

Both anti-ubiquitin antibodies Ub-Fl76 and Ubi-1 detected signature neuronal intranuclear inclusions (NII) in neurons of the R6/2 mouse model of Huntington's disease but not in normal control mouse brains.

Results.

Hap40 Immunoblotting.

Immunoblotting of Hela cell extracts with the anti-Hap40 antibody revealed a band at the expected molecular weight of 40 kDa (Figure 1 a). Mouse brain protein extracted with reducing, SDS containing buffer revealed a doublet at ~30kDa consisting of major and minor bands of lower and higher electrophoretic mobility respectively (Figure 1 b, lane 1). A similar Hap40 immunoreactive doublet was detected using this antibody by Pal et al. in Hap40/Huntingtin enriched bovine brain lysate eluted from a Rab5-GTP affinity column (Pal et al., 2006). The higher electrophoretic mobility band intensity was dramatically reduced in brain protein extracted with non-reducing Triton X-100 containing buffer (Figure 1 b, lane 2) and could only be detected upon overexposure. The reason for the difference in the apparent molecular weight of Hap40 immunoreactive signal in the cell line and the brain extracts is uncertain and may reflect differential post-translational modifications of the protein among these two systems.

Subcellular localization of Hap40-like immunoreactivity in mouse brain.

At the cellular level, immunostaining of mouse brain sections for Hap40 revealed three distinct patterns of immunoreactivity. Consistent with previous descriptions of Hap40 nuclear staining in cultured cells (9), many neurons displayed innumerable small intensely immunoreactive intranuclear dots, producing a diffuse or punctate pattern of nuclear immunoreactivity (Figure 2 a, c). In other neurons, diffuse or granular cytoplasmic staining was observed (Figure 2 d, f). Finally, some cells displayed solitary, bright, sharply-defined

Figure 1. Western blot analysis of Hap40-like immunoreactivity in HeLa cell lysate and mouse brain protein extract.

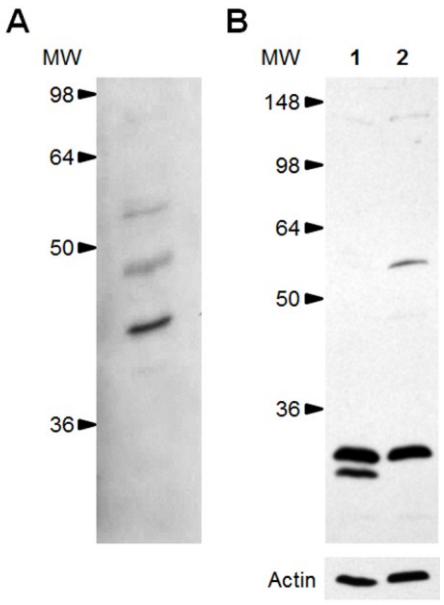

Legend to Figure 1. Western blot analysis of Hap40-like immunoreactivity in HeLa cell lysate and mouse brain protein extract.

Western blot analysis probed with anti-Hap40 antibodies of (A) HeLa cell lysate showing a ~40kDa band and (B) of mouse brain protein extracted with either 2% SDS/5% -mercaptoethanol containing buffer (lane 1 in B) or a milder 1% Triton X-100 containing buffer (lane 2 in B) showing either a doublet or a single band at ~30kDa respectively. Blot was stripped and re-probed for actin as a loading control (bottom panel in B).

Figure 2. Patterns of Hap40-like immunoreactivity in the mouse brain.

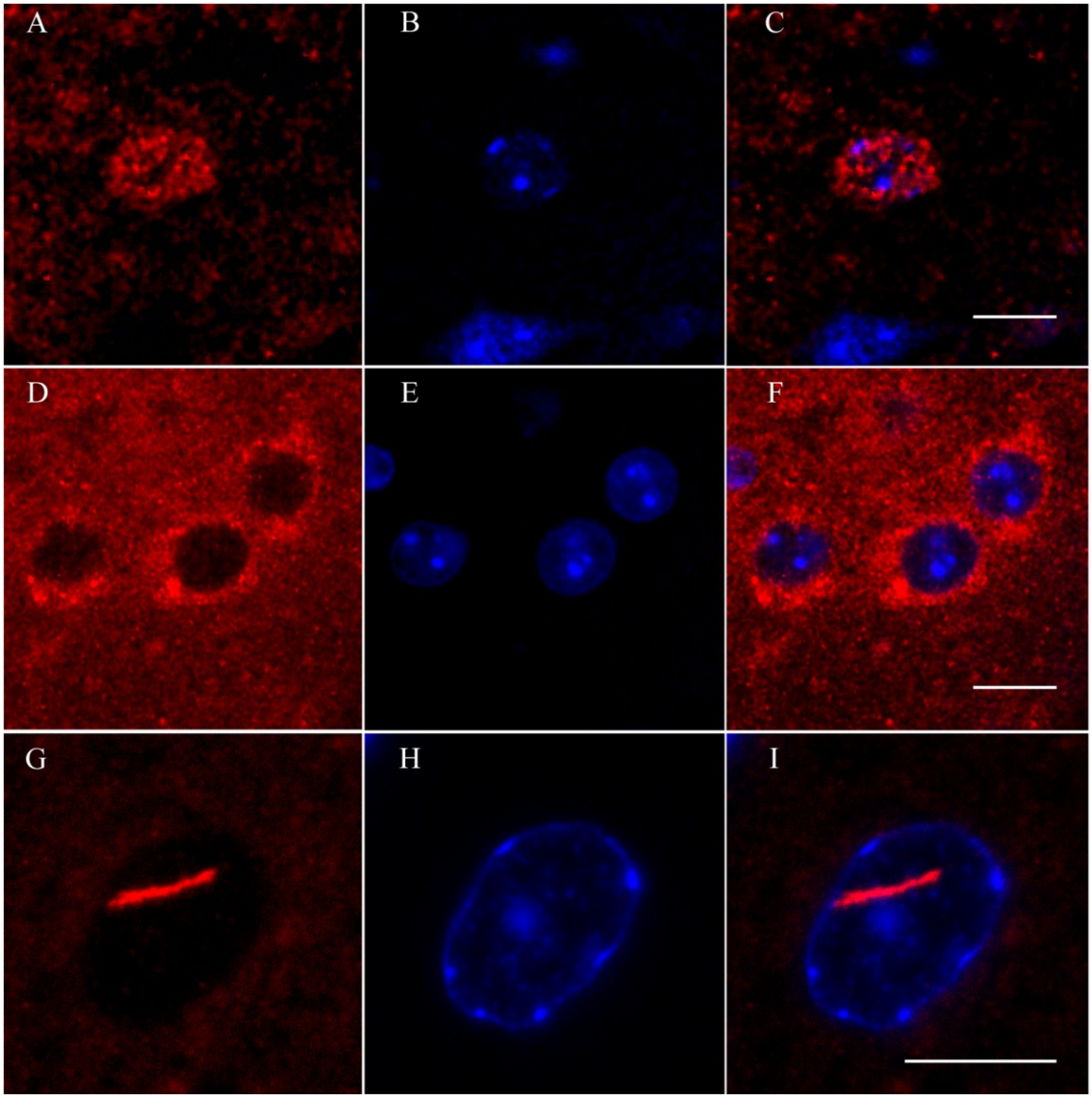

Legend to Figure 2. Patterns of Hap40-like immunoreactivity in the mouse brain.

Hap-40 immunofluorescence in CD1 mouse brain sections using antibody ab5872 (A, D, G) counterstained with DAPI nuclear stain (B, E, H). Merged images shown in C, F, I. A - C) Punctate nuclear Hap40 staining pattern in a cerebral cortical neuron. D-F) predominantly cytoplasmic distribution of Hap40 immunoreactivity in thalamic neurons. G-I) Hap40-INR in a hypothalamic neuron. Scale bars=10μm.

intranuclear structures which will be referred to as HAP40-INRs (Figure 2 g, i). These ranged from small, dot or bar-like structures measuring roughly 0.5μm in diameter to long, rod-shaped structures that sometimes spanned the entire diameter of the nucleus. The diffuse or punctate pattern of nuclear and/or cytoplasmic Hap40-like immunoreactivity was observed throughout the brain. However, Hap40-INRs displayed a highly selective topographic pattern of localization. Equivalent observations were made using two distinct polyclonal antisera against Hap40 (see Table 1 for antibody source).

Although rare scattered Hap40-INRs were identified throughout the brain including olfactory bulb, lateral septum, cerebellum and occasionally in CA3 neurons of the hippocampus, they were invariably and most abundantly found in the posterior lateral hypothalamus (lateral hypothalamic area and zona incerta, further cumulatively referred to as LHA), the lateral parabrachial nucleus and the locus coeruleus (LC) (Table 2). Therefore most of our subsequent investigations focused on these brain regions.

Hap40-INRs are not immunoreactive with antisera against Huntingtin or Huntingtin associated protein 1 (Hap1).

To investigate whether other huntingtin associated proteins are present within Hap40-INRs and given that Hap40 is known to functionally and physically interact with the huntingtin protein itself (Pal et al., 2006; Peters and Ross, 2001), we double stained mouse brain sections with antisera against Hap40 and either huntingtin or the huntingtin associated protein 1 (Hap1). We did not detect Hap1 or huntingtin localization to Hap40-INRs in the hypothalamus or the LC.

Table 2. Relative abundance of Hap40- and Ub-Fl76-INRs in mouse brain.

Brain Region	Hap40-INRs	Ub-Fl76-INR
Olfactory bulb	+/-	N/A
Lateral septum	++	N/A
Lateral hypothalamic area	+++*	+++
Arcuate nucleus of hypothalamus:		
Dorsolateral aspect	+/-	+
Ventromedial aspect	-	+
Locus coeruleus	+++	+++
Cerebellum	+/-	+/-

+/- sometimes observed; - never observed; + signs indicate relative prevalence of INRs in a given brain area; N/A not assessed. * only in melanin concentrating hormone immunoreactive neurons.

Hap40-INRs contain ubiquitinated proteins.

We have previously shown that a subset of SDL-INRs in the pigmented neurons of the human substantia nigra (SN) are immunoreactive for ubiquitin and promyelocytic leukemia (PML) protein (Woulfe et al., 2004). Berciano et al reported PABPN1-INRs to be immunoreactive with antibodies to ubiquitin and the 19S (and to a considerably lesser extent the 20S) proteasomal subunit (Berciano et al., 2004). We therefore tested Hap40-INRs for PML, ubiquitin and 19S immunoreactivity.

No PML immunoreactivity associated with Hap40-INRs could be demonstrated in the mouse brain using two different commercially available antibodies (Table 1).

Next, using a polyclonal anti-ubiquitin antibody (Ub-Fl76; Table 1) we detected intensely immunoreactive INRs in all brain areas and cell types where Hap40-INRs were originally identified (Figure 3, 5 and 7). However, Ub-Fl76 immunoreactive INRs exhibited a wider distribution than that of Hap40-INRs. In particular, Ub-Fl76 immunoreactive INRs were prevalent in the arcuate nucleus (Arc) and the ventro-medial hypothalamus where Hap40-INRs were rarely observed. Double immunofluorescence using Hap40 and Ub-Fl76 antibodies could not be performed since both antisera were raised in rabbit. We, therefore, performed double immunofluorescence staining using a mouse monoclonal anti-ubiquitin antibody (Ubi-1, Table 1) in combination with either the Hap40 antibody or the Ub-Fl76 antibody. Ubi-1 antibody was reported by the manufacturer to recognize "polyubiquitin chains much more strongly than monoubiquitinated molecules or free ubiquitin". Ubi-1 double staining of INRs was observed with both the Hap40 and the Ub-Fl76 antibodies (Figure 3). However, unlike UbFl76, Ubi-1 staining of INRs was partial and discontinuous, consisting of a linear array of dots or bar-shaped structures, overlapping portions of the INR as delineated by continuous Hap40 or Ub-Fl76

Figure 3. Ubiquitinated proteins in INRs.

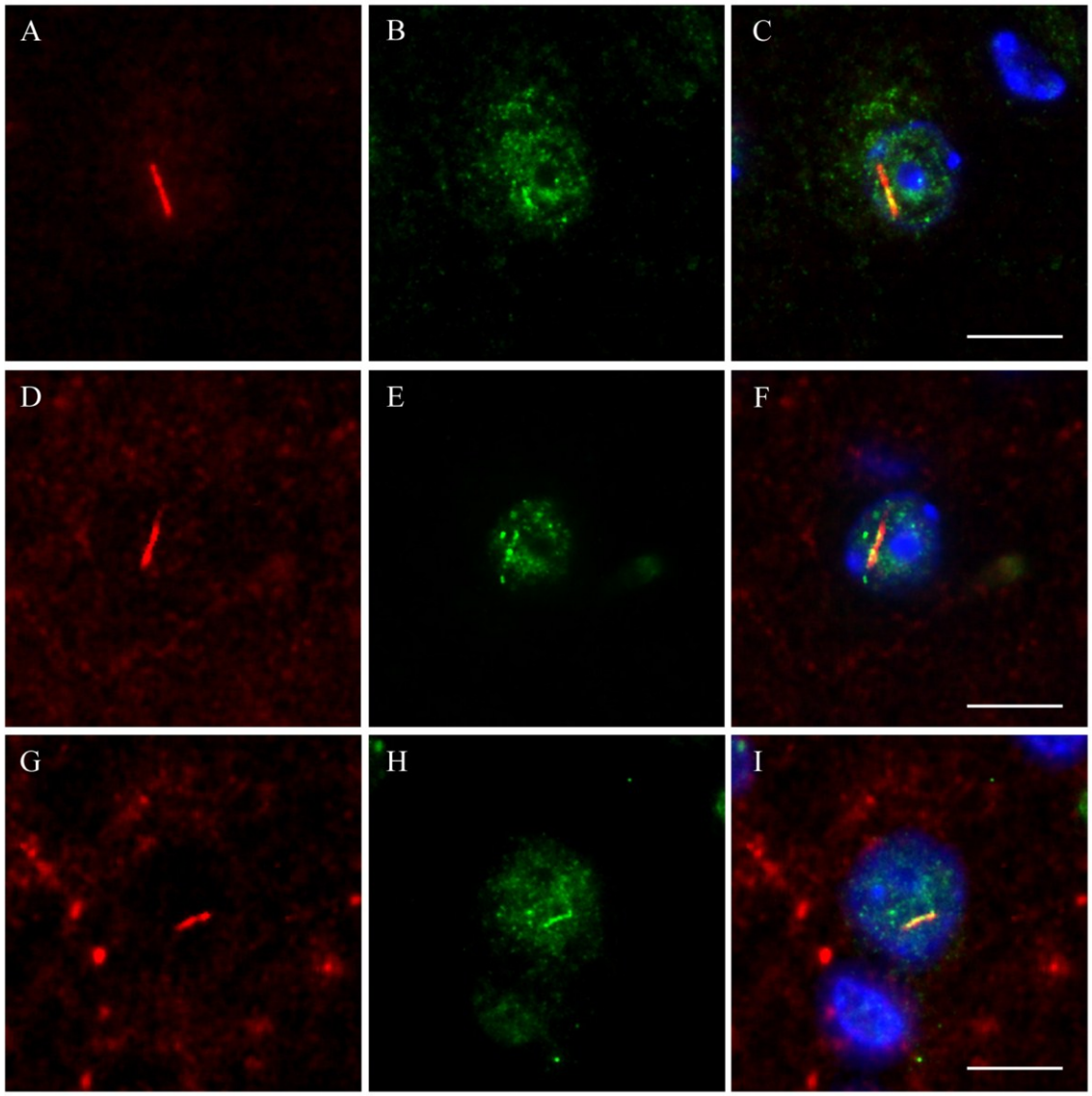

Legend to Figure 3. Ubiquitinated proteins in INRs.

Double immunofluorescence staining using the anti-ubiquitin Ubi-1 antibody (B, E, H) combined with either anti-Hap40 antibody ab5872 (A) or anti-ubiquitin antibody Ub-Fl76 (D, G). C, F, I) Merged images counterstained with DAPI. A-C and D-F) Typical pattern of partial overlap of Ubi-1 immunoreactivity with Ub-Fl76 and Hap40-INR, respectively. G, H, I) Less commonly encountered instance of extensive Ubi-1 labelling of a Hap40-INR. Scale bars=10μm.

staining (Figure 3, a to f). Some continuous INR staining was also observed, particularly in the LHA and LC (Figure 3, g to i). This ubiquitin immunoreactivity prompted us to investigate a possible recruitment of the proteasomal proteolytic machinery to ubiquitin immunoreactive INRs. Berciano et al. reported intense immunoreactivity of ubiquitin immunoreactive, PABPN-INR using a commercially available antibody to the Rpt5 subunit of the regulatory 19S proteosomal subunit. We did not detect 19S recruitment to Ub-Fl76 immunoreactive INRs using this antibody.

Selective localization of Hap40- and ubiquitin immunoreactive INR to specific neuronal subpopulations.

Hap40-INRs were observed in several regions of the brain. Within some of these regions Hap40-INRs were further confined to specific neurochemically-defined neuronal populations. This selectivity was exemplified in the hypothalamus where in LHA Hap40-INRs were localized exclusively to neurons showing cytoplasmic immunoreactivity for melanin-concentrating hormone (MCH) (Figure 4 a and c) and were excluded from orexin-containing neurons (Figure 4 b and d), which are located in the same region and intermingle with MCH neurons. In order to assess the prevalence of Hap40-INR in MCH immunoreactive neurons quantitative analysis of hypothalamic sections from 15 wt CD-1 mice (8 females and 7 males) were double stained for MCH and Hap40-INR. Hap40-INR frequency ranged from 11.1% to 71.4% with a mean of 44.0±4.9% of MCH neurons containing Hap40-INRs. When examined separately, there was no significant difference in Hap40-INR frequency among male and female mice (41.6±7.9% vs. 46.1±6.4% respectively).

Figure 4. Exclusive localization of Hap40-INRs of the LHA to MCH positive neurons.

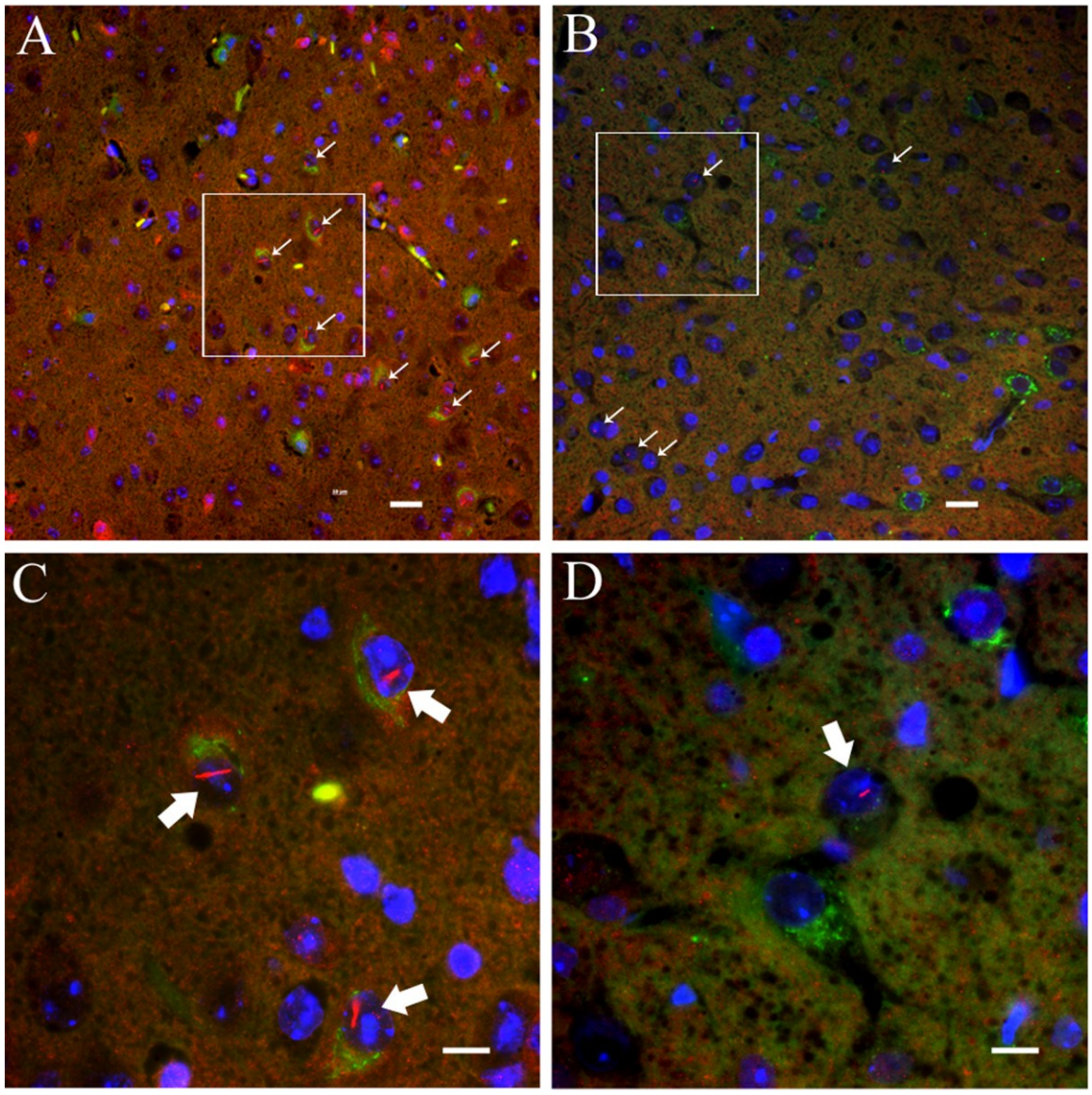

Legend to Figure 4. Exclusive localization of Hap40-INRs of the LHA to MCH positive neurons.

Double immunofluorescence staining of mouse hypothalamus with anti-Hap40 antibody ab5872 combined with either an anti-pro-MCH antibody (A) or anti-orexin antibody (B) and DAPI counterstain. C, D) Higher magnification images of the boxed regions in A and B, respectively. Arrows indicate Hap40-INR containing nuclei. Note Hap40-INR localization to MCH positive neurons and exclusion from orexin positive cells. Scale bars=20μm in A and B; 10μm in C and D.

In light of the wider distribution of Ub-Fl76 immunoreactive INRs relative to Hap40-INRs, we examined whether a similar selective relationship existed between Ub-Fl76-INRs and hypothalamic MCH and orexin neurons. Double labelling immunofluorescence for ubiquitin and either orexin or MCH showed that, like Hap40-INRs, Ub-Fl76-INRs were present in MCH neurons at a similar frequency (45.2±5.4%, n=4) (Figure 5 a, c) but were excluded from orexin neurons (Figure 5 b, d). In addition, a substantial fraction of hypothalamic Ub-Fl76-INRs were present in MCH negative neurons and these were concentrated in the arcuate nucleus, ventro-medial hypothalamic nucleus and ventral part of the premammillary nucleus.

By analogy with the differential localization of Hap40-INRs in MCH versus orexin neurons in the LHA, we wondered whether there might be a differential localization of Ub-Fl76 immunoreactive INRs in pro-opiomelanocortin (POMC) versus neuropeptide Y (NPY) expressing neurons in the arcuate nucleus. Anti-POMC immunofluorescence staining allowed for clear identification of immunoreactive neuronal cell bodies. Ub-Fl76-INRs were found in both the POMC positive and the POMC negative neurons of the arcuate nucleus (Figure 6). Immunofluorescence staining for NPY revealed numerous brightly stained neuronal processes. However, in the absence of colchicine pre-treatment, no NPY immunoreactive cell bodies could be demonstrated.

Both Hap40-INRs and Ub-Fl76-INRs were prevalent in LC neurons. Double-staining immunofluorescence for ubiquitin and TH confirmed that Ub-Fl76-INRs were localized exclusively to TH immunoreactive noradrenergic LC neurons (Figure 7). In addition, adjacent serial sections through the LC of 4 mice were single stained for TH, Hap40- and Ub-Fl76-INR. Quantification of TH-positive neurons, Hap40-INRs and Ub-Fl76-INRs in respectively stained sections revealed a considerable degree of inter-individual variability. The ratio of Hap40-INR to

Figure 5. Selective localization of Ub-INRs in the LHA.

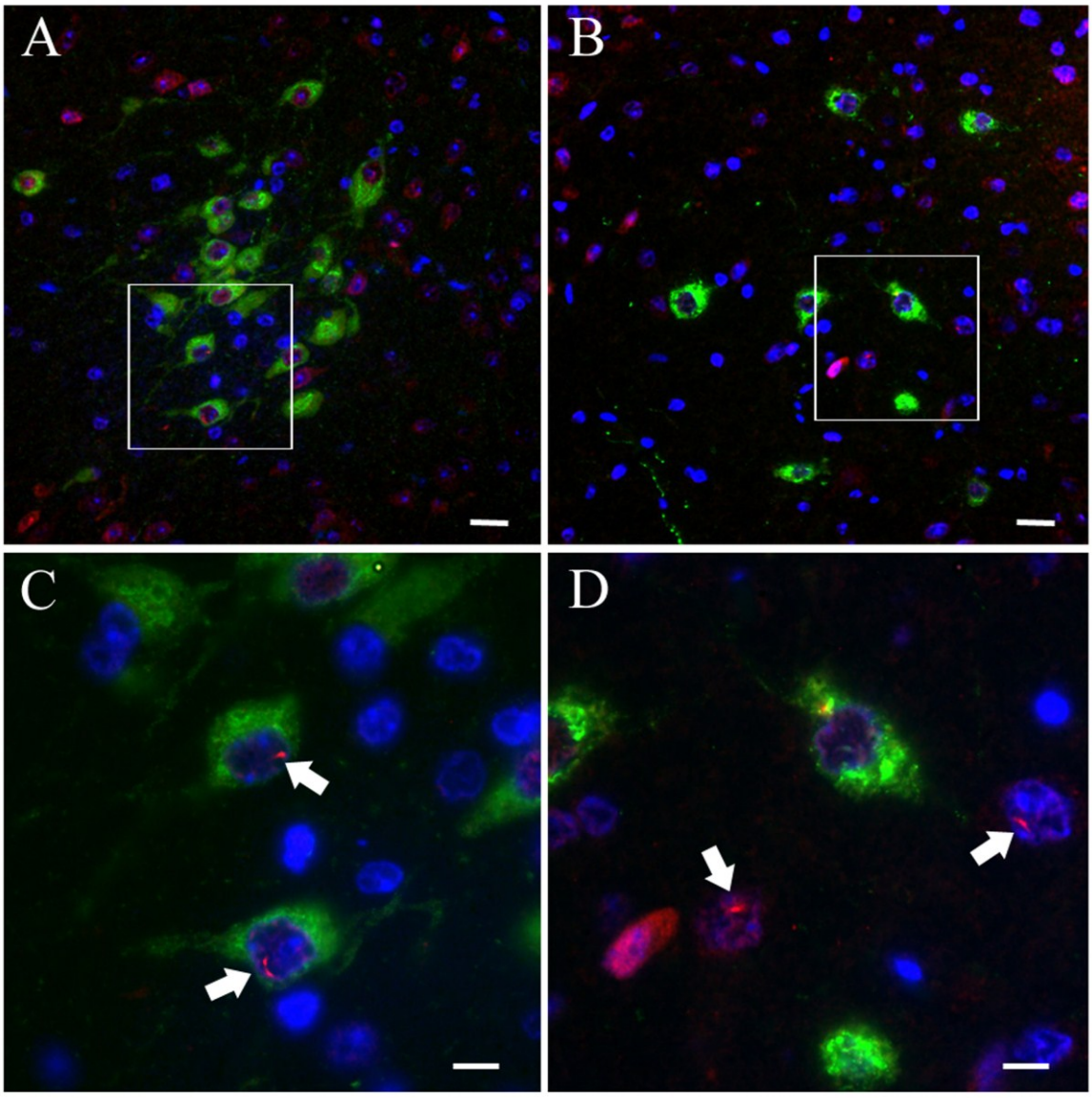

Legend to Figure 5. Selective localization of Ub-INRs in the LHA.

Double immunofluorescence staining of mouse hypothalamus with anti-ubiquitin antibody Ub-Fl76 and either an anti-pro-MCH antibody (A) or anti-orexin antibody (B) and DAPI counterstain. C, D) Higher magnification images of the boxed regions in A and B, respectively. Arrows indicate Ub-INR containing nuclei. Note Ub-INR localization to MCH positive neurons and exclusion from orexin positive cells. Scale bars=20μm in A and B; 10μm in C and D.

Figure 6. Localization of Ub-INRs in relation to POMC neurons in the Arcuate nucleus of hypothalamus.

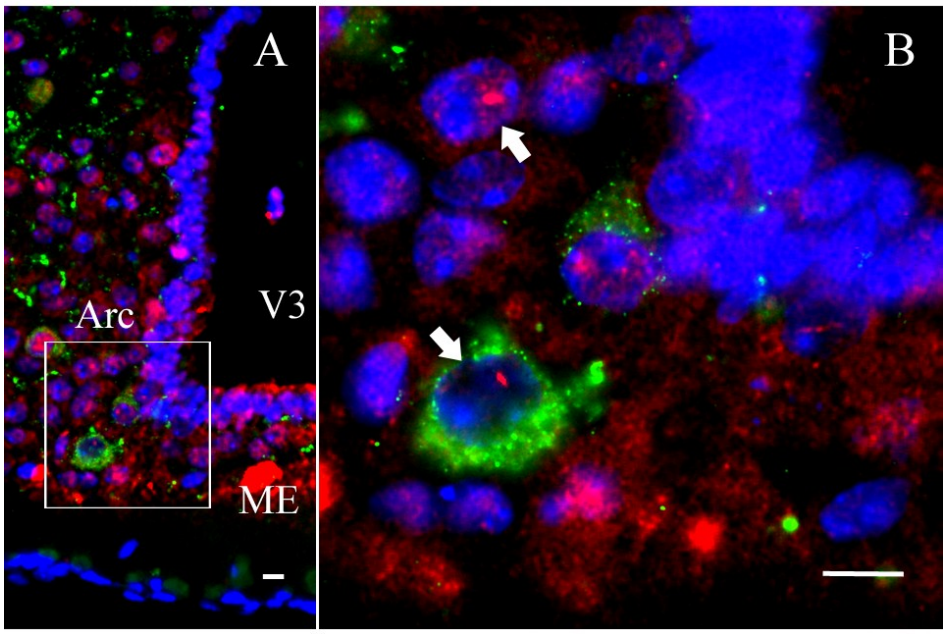

Legend to Figure 6. Localization of Ub-INRs in relation to POMC neurons in the Arcuate nucleus of hypothalamus.

Double immunofluorescence staining of mouse hypothalamus with anti-ubiquitin antibody Ub-Fl76 and an anti-POMC antibody with DAPI counterstain. A) Lower magnification micrograph including the arcuate nucleus (Arc), median eminence (ME), and third ventricle (V3). B) Higher magnification image of the boxed region in A. Arrows point to Ub-INR containing nuclei. Note presence of Ub-INR in both POMC positive and negative cells. Scale bars=10μm.

Figure 7. Localization of Ub-INRs to TH positive neurons in Locus Coeruleus.

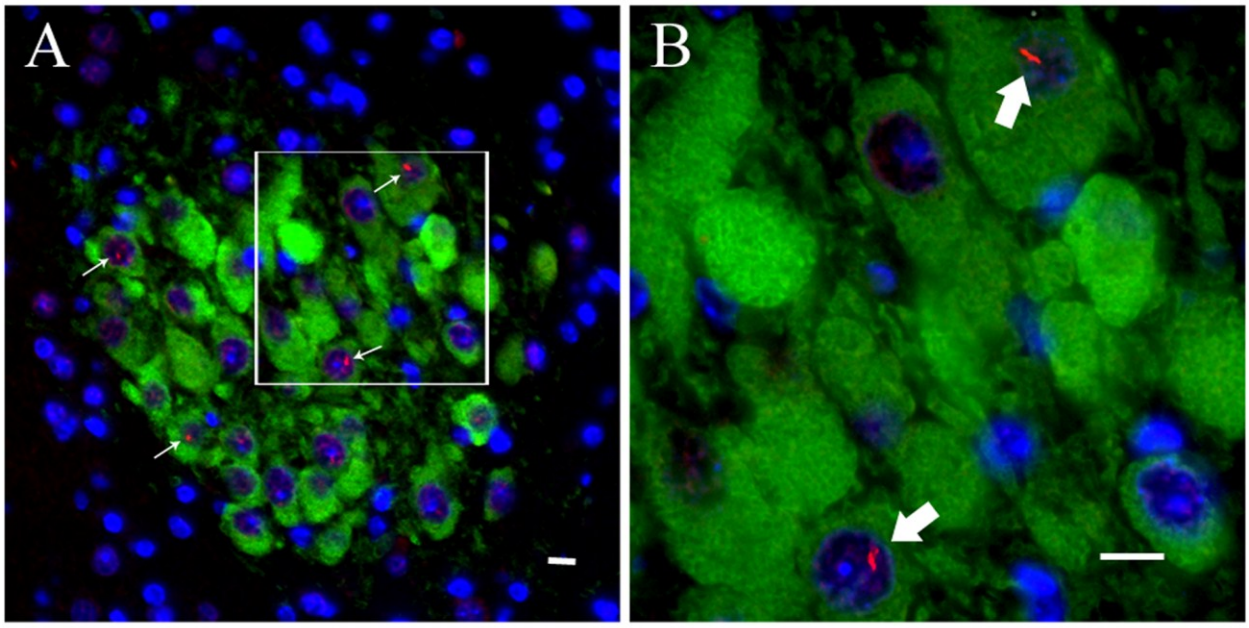

Legend to Figure 7. Localization of Ub-INRs to TH positive neurons in Locus Coeruleus.

Double immunofluorescence staining of mouse locus coeruleus with anti-ubiquitin antibody Ub-Fl76 and anti-TH antibody and DAPI counterstain. A) Low magnification image of the LC. B) Higher magnification of the boxed region in A. Arrows indicate Ub-INR containing nuclei. Note the localization of Ub-INRs to TH positive neurons. Scale bars=10μm.

TH positive neuron counts ranged from zero to 0.641 with a mean of 0.338±0.143. Similarly, the ratio of Ub-Fl76-INR to TH positive neurons ranged from zero to 1 with a mean of 0.536±0.218.

Spatial relationship between Hap40-INR and SDL-INR.

We have previously described the distribution of SDL-INRs in human brain (Woulfe and Munoz, 2000). In the present study, we identified SDL-INRs in all areas of mouse brain containing Hap40-INRs. In these areas, SDL-INRs were far more numerous than either Hap40- or Ub-Fl76-INRs. Notably, in the LHA all Hap40-INR containing MCH neurons also contained an SDL-INR within the same nucleus (Figure 8 a-c). In these neurons the Hap40- and SDL-INR were typically found in close juxtaposition, each exhibiting continuous, uninterrupted staining (Figure 8 g, h). INRs containing intermittent Hap40 and SDL.3D10 staining were not observed. This contrasted sharply with the mutually exclusive relative distribution of Hap40- and SDL-INRs in the LC where Hap40-INRs were found in magnocellular neurons, while SDL-INRs were found in smaller cells (Figure 8, d-f and i).

Figure 8. Topographic and cellular distribution of Hap40- and SDL-INRs in mouse hypothalamus and locus coeruleus.

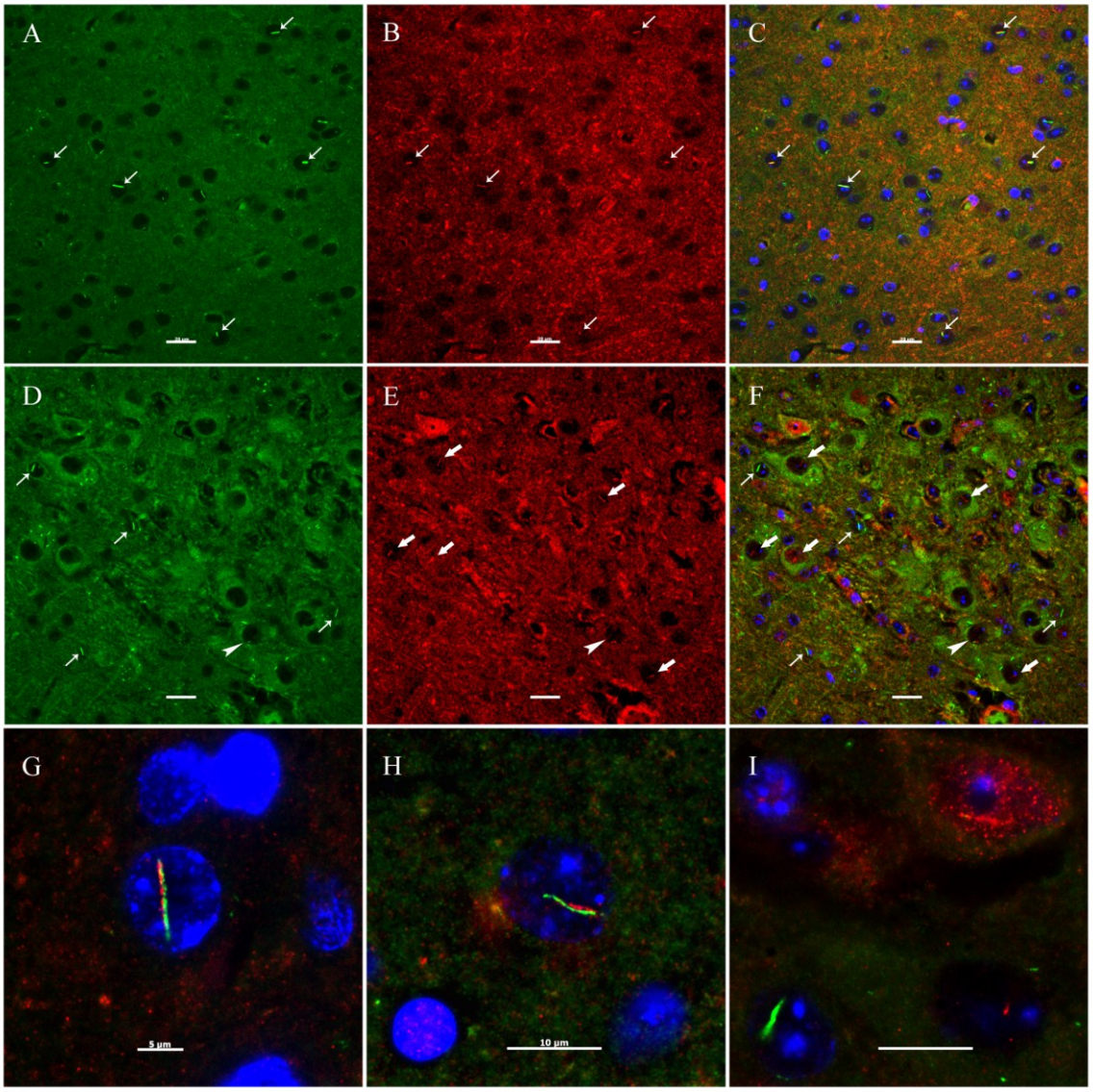

Legend to Figure 8. Topographic and cellular distribution of Hap40- and SDL-INRs in mouse hypothalamus and locus coeruleus.

Non-random spatial distribution of Hap40-INRs (red) and SDL-INRs (green) in mouse hypothalamus (A, B, C, G, H) and locus coeruleus (D, E, F, I). In the hypothalamus, all Hap40-INR containing nuclei (arrows in B and C) also contain an SDL-INR (arrows in A and C). In these neurons, despite close spatial juxtaposition, Hap40- and SDL-INRs appear as distinct entities (G, H). In the locus coeruleus, Hap40-INRs are confined to magnocellular neurons (thick arrows in E and F). In contrast, SDL-INRs are found in smaller cells (thin arrows in D and F). A higher magnification image of Hap40- and SDL-INR in the locus coeruleus is shown in I. Arrowhead in D, E and F points to a rare magnocellular neuron in the locus coeruleus containing both a Hap40-INR and a small SDL-INR. Scale bars=20μm in A-F; 5μm in G; and 10μm in H and I.

Discussion.

First reported in the late 1800's, INRs are among the earliest documented intranuclear structures. Nevertheless, they remain amongst the least understood nuclear bodies. To this day INRs are identified principally on the basis of their unique morphological and ultrastructural features as observed by light and electron microscopy. Until recently, INRs were presumed to comprise a biochemically and functionally homogeneous class of nuclear bodies. This view was challenged in 2004 by Berciano and colleagues who reported intranuclear structures in rat supraoptic nucleus neurons that could be identified morphologically and ultrastructurally as INRs but did not immunostain with SDL.3D10. Instead these structures were intensely immunoreactive for PABPN1. Although both PABPN1- and SDL-INRs were present in rat SON, they displayed a differential and mutually exclusive distribution with PABPN1-INRs confined to oxytocinergic neurons and SDL-INRs found in vasopressin-containing neurons (Berciano et al., 2004). This indicated that INRs may represent a family of morphologically homogeneous, but biochemically diverse intranuclear structures that are differentially distributed among neurochemically and/or functionally distinct neuronal subpopulations.

In the present study, we confirmed and extended this concept of INR diversity by describing a new subtype of INR displaying Hap40-like immunoreactivity, and by providing evidence for the existence of additional INR subtypes whose defining protein constituents remain to be identified but which share ubiquitin immunoreactivity as a common feature.

Isolated in 2001 by Peters and Ross (Peters and Ross, 2001), Hap40 is one of a long list of proteins that have been shown to interact with the Huntington's disease (HD) protein, huntingtin (1993). Endogenous Hap40 shows a dual subcellular localization. Its amino acid sequence contains a nuclear localization signal-like sequence, mutation of which diminished nuclear

localization of a Hap40-GFP fusion protein. Huntingtin itself may have a role in Hap40 nuclear targeting. HEK293 cells co-transfected with Hap40 and huntingtin showed cytoplasmic co-localization of both proteins. However, in the absence of huntingtin, exogenous Hap40 showed a nuclear localization. The Hap40 nuclear staining pattern in transfected cells was either diffuse or appeared as punctate nuclear structures which did not correspond to splicing speckles or PML bodies (Peters and Ross, 2001). We encountered both of these patterns of immunoreactivity for endogenous Hap40 protein in mouse brain sections. In addition, in select brain areas, we observed distinct, Hap40 immunoreactive rod shaped nuclear structures which we have termed Hap40-INRs. These structures did not stain for PML and therefore are not related to PML bodies. Nor did we detect huntingtin immunoreactivity within INRs.

Hap40 is an effector of the small GTPase Rab5, a key regulator of endocytosis. It mediates the recruitment of huntingtin by Rab5 onto early endosomes. The Hap40-huntingtin complex on endosomes subsequently displaces them from microtubules and enhances their affinity for actin, thereby resulting in reduced endosomal motility (Pal et al., 2006). The presence of Hap40-like immunoreactivity within the nucleus and in INRs raises questions regarding the potential function and interacting partners of nuclear Hap40, which to date have not been reported. It is noteworthy that a number of endosomal proteins, including effectors of Rab5, APPL1 and APPL2, have a dual cytoplasmic and nuclear localization (Miaczynska et al., 2004a). Interestingly, another endosomal protein that is also a huntingtin associated protein, Hap1, was previously reported to localize to distinct nuclear rod shaped structures (Gutekunst et al., 1998); although, we did not detect its association with Hap40-INRs. Like Hap40, the Hap1/huntingtin complex is involved in vesicular trafficking and perturbed Hap1/huntingtin interaction leads to a trafficking defect with consequent neurodegeneration (Block-Galarza et al., 1997; Engelender et al., 1997; Gauthier et al., 2004). According to an emerging hypothesis, by translocating to the

nucleus, endosomal vesicle-associated proteins could act as signalling molecules to co-ordinate endocytic events at the plasma membrane with appropriate alterations in gene expression in the nucleus (Miaczynska et al., 2004b). The pattern of ubiquitin immunoreactivity we have described may be relevant in this regard. We observed continuous, uninterrupted labelling of INR with the Ub-Fl76 antibody, which recognizes both mono- and polyubiqutin. In contrast, partial, dot or bar like INR staining was typically observed with the Ubi-1 antibody, a monoclonal antibody with a strong preference for polyubiquitin chains. Although it remains to be demonstrated conclusively, this suggests that ubiquitin immunoreactivity in INRs may reflect the presence of predominantly monoubiquitnated protein. The lack of detectable levels of 26S proteasome on INRs would also be more consistent with a non-proteolytic regulatory function associated with INR ubiquitination. Monoubiquitination of endocytic adapter proteins is a crucial post-translational modification which regulates their ability to bind to ubiquitinated substrates, such as endocytosed activated membrane receptors (Hoeller et al., 2006). Monoubiquitination also regulates nuclear versus cytoplasmic localization and consequently transcriptional activity of a number of transcription factors (Carter et al., 2007; van der Horst et al., 2006). Monoubiquitination of other nuclear proteins, for example the histones H2A and H2B, has also been demonstrated to play an important role in transcriptional regulation (Minsky et al., 2008; Zhou et al., 2008). It is tempting to speculate that the monoubiquitination of certain proteins, such as Hap40, could provide a mechanistic link between endosomal tethering, nucleocytoplasmic trafficking and transcriptional regulation. In this context, recruitment of ubiquitinated proteins to INRs may reflect a specialized aspect of such signalling regulation within select neuronal subpopulations.

As was previously described for SDL-INRs in human brain (Woulfe 2000) and for PABPN1-INRs in rat SON (Berciano 2004), Hap40-INRs display a stereotypic pattern of

distribution in the mouse brain. In certain brain regions, Hap40-INRs are confined to specific neurochemically and/or anatomically defined neuronal subpopulations implying that these structures have a specialized functional role in these neurons. Orexinergic and MCH neurons of the LHA give rise to extensive efferent axonal projections with targets throughout the brain and are involved in the regulation of sleep/wakefulness, appetite and locomotor activity (Burdakov 2005). Despite their intimate anatomical proximity, the orexin and MCH neurons are antagonistic with respect to many of their physiological functions. The selective association of Hap40-INRs with MCH neurons and their exclusion from orexin neurons represents yet another point of divergence among these two neuronal populations. By analogy with orexin and MCH neurons in the LHA, POMC and NPY neurons of the arcuate nucleus have antagonistic roles, wherein POMC neurons inhibit feeding and stimulate energy expenditure while NPY neurons stimulate food intake and inhibit energy expenditure. Although technical limitations precluded us from examining the differential localization of Ub-INRs in NPY neurons, we were able to demonstrate them in POMC neurons. The presence of Hap40-INRs in the LHA and Ub-INRs in the LHA and the arcuate nucleus allows for a possible role for these structures in central regulation of metabolism.

Both Hap40- and Ub-INRs were readily detectable in the LC where they selectively localized to the magnocellular LC neurons. These neurons have widely divergent, long-range, branching efferent projections throughout the brain providing noradrenergic input to virtually all brain areas (Sara, 2009). In this respect, LC neurons are similar to MCH and POMC neurons, which also have extremely divergent, long-range, branching efferent projections. The possibility that Hap40/Ub-INRs represent morphological markers of this type of neuron is worthy of consideration and would support the concept of a role for these structures in integration of long range vesicular transport with dynamic regulation of nuclear gene expression.

In this study we also examined a relationship between the classical SDL-INRs and the newly described Hap40- and Ub-INRs. The nature of this relationship varied among neuronal populations. Thus, SDL-INRs were typically excluded from Hap40- or Ub-INR containing neurons of the LC whereas all Hap40-INR-containing MCH neurons also contained an SDL-INR in the same nucleus. Furthermore, a non-random spatial association existed between the two types of INR within a single nucleus whereby Hap40- and SDL-INRs were aligned in close juxtaposition along their long axes. The intimate association of the two distinct INR-subtypes raises several interesting questions including the mechanism underlying the differential recruitment of INR subtype-specific protein to its cognate INR scaffold. Since this study constitutes the first report of co-existence of biochemically distinct INRs within the same nucleus, the definitive answer to this question will require further investigation.

Finally, the relative anatomical distribution of Hap40- and Ub-INRs is of particular interest. The absence of Hap40-INRs from specific brain regions containing abundant Ub-INRs points to the existence of additional INR subtypes containing yet to be defined ubiquitinated protein(s).

Our morphological data should serve as a prelude to further investigation of a functional relationship between INRs and neuronal function. The differential association of biochemically distinct INR subtypes with neurochemically and/or anatomically defined neuronal cell populations suggests a specific requirement for a given INR subtype within specific identifiable neuronal populations. Future studies will examine possible involvement of these structures in neuropathological disorders targeting these specific cell populations. For example, by analogy with the loss of SDL-INRs from cortical neurons in Alzheimer's disease, Hap40- and/or Ub-INRs may be involved in the pathogenesis of metabolic disorders involving the central hypothalamic regulation of energy homeostasis and food intake.

Conflict of Interest Statement.

There is no known or potential conflict of interest (including any financial, personal or other relationships with other people or organizations) that could inappropriately influence, or be perceived to influence, the findings described in this article.

Role of authors.

All authors had full access to all the data in the study and take responsibility for the integrity of the data and the accuracy of the data analysis. Study concept and design: John Woulfe and Pavel Milman. Acquisition of data: Pavel Milman. Analysis and interpretation of data: John Woulfe and Pavel Milman. Drafting of the manuscript: Pavel Milman. Critical revision of the manuscript for important intellectual content: John Woulfe. Statistical analysis: Pavel Milman. Obtained funding: John Woulfe.

References.

1993. A novel gene containing a trinucleotide repeat that is expanded and unstable on Huntington's disease chromosomes. The Huntington's Disease Collaborative Research Group. Cell 72(6):971-983.

Banerjee A, Roach MC, Trcka P, Luduena RF. 1990. Increased microtubule assembly in bovine brain tubulin lacking the type III isotype of beta-tubulin. J Biol Chem 265(3):1794-1799.

Berciano MT, Villagra NT, Ojeda JL, Navascues J, Gomes A, Lafarga M, Carmo-Fonseca M. 2004. Oculopharyngeal muscular dystrophy-like nuclear inclusions are present in normal magnocellular neurosecretory neurons of the hypothalamus. Hum Mol Genet 13(8):829-838.

Block-Galarza J, Chase KO, Sapp E, Vaughn KT, Vallee RB, DiFiglia M, Aronin N. 1997. Fast transport and retrograde movement of huntingtin and HAP 1 in axons. Neuroreport 8(9-10):2247-2251.

Broberger C, De Lecea L, Sutcliffe JG, Hokfelt T. 1998. Hypocretin/orexin- and melanin-concentrating hormone-expressing cells form distinct populations in the rodent lateral hypothalamus: relationship to the neuropeptide Y and agouti gene-related protein systems. The Journal of comparative neurology 402(4):460-474.

Bullmann T, Hartig W, Holzer M, Arendt T. Expression of the embryonal isoform (0N/3R) of the microtubule-associated protein tau in the adult rat central nervous system. The Journal of comparative neurology 518(13):2538-2553.

Cajal SR. 1909. Histologie du systeme nerveux de l'homme et des vertebres. Consejo Superior de Investigaciones Cientificas, Madrid 1.

Carter S, Bischof O, Dejean A, Vousden KH. 2007. C-terminal modifications regulate MDM2 dissociation and nuclear export of p53. Nat Cell Biol 9(4):428-435.

Deurveilher S, Lo H, Murphy JA, Burns J, Semba K. 2006. Differential c-Fos immunoreactivity in arousal-promoting cell groups following systemic administration of caffeine in rats. The Journal of comparative neurology 498(5):667-689.

Engelender S, Sharp AH, Colomer V, Tokito MK, Lanahan A, Worley P, Holzbaur EL, Ross CA. 1997. Huntingtin-associated protein 1 (HAP1) interacts with the p150Glued subunit of dynactin. Hum Mol Genet 6(13):2205-2212.

Gauthier LR, Charrin BC, Borrell-Pages M, Dompierre JP, Rangone H, Cordelieres FP, De Mey J, MacDonald ME, Lessmann V, Humbert S, Saudou F. 2004. Huntingtin controls neurotrophic support and survival of neurons by enhancing BDNF vesicular transport along microtubules. Cell 118(1):127-138.

Gray EG, Guillery RW. 1963. An Electron Microscopical Study of the Ventral Nerve Cord of the Leech. Z Zellforsch Mikrosk Anat 60:826-849.

Gutekunst CA, Li SH, Yi H, Ferrante RJ, Li XJ, Hersch SM. 1998. The cellular and subcellular localization of huntingtin-associated protein 1 (HAP1): comparison with huntingtin in rat and human. J Neurosci 18(19):7674-7686.

Hoeller D, Crosetto N, Blagoev B, Raiborg C, Tikkanen R, Wagner S, Kowanetz K, Breitling R, Mann M, Stenmark H, Dikic I. 2006. Regulation of ubiquitin-binding proteins by monoubiquitination. Nat Cell Biol 8(2):163-169.

Lamba W, Prichett W, Munoz D, Park DS, Woulfe JM. 2005. MPTP induces intranuclear rodlet formation in midbrain dopaminergic neurons. Brain Res 1066(1-2):86-91.

Lessard JL. 1988. Two monoclonal antibodies to actin: one muscle selective and one generally reactive. Cell Motil Cytoskeleton 10(3):349-362.

Marinesco G. 1902. Sur la presence des corpuscles acidophiles paranucleolaires dans les cellules du locus niger et du locus ceruleus. Compt Rend Acad Sci 135:1000-1002.

Masurovsky EB, Benitez HH, Kim SU, Murray MR. 1970. Origin, development, and nature of intranuclear rodlets and associated bodies in chicken sympathetic neurons. J Cell Biol 44(1):172-191.

Miaczynska M, Christoforidis S, Giner A, Shevchenko A, Uttenweiler-Joseph S, Habermann B, Wilm M, Parton RG, Zerial M. 2004a. APPL proteins link Rab5 to nuclear signal transduction via an endosomal compartment. Cell 116(3):445-456.

Miaczynska M, Pelkmans L, Zerial M. 2004b. Not just a sink: endosomes in control of signal transduction. Curr Opin Cell Biol 16(4):400-406.

Milman P, Fu A, Screaton RA, Woulfe JM. 2010. Depletion of intranuclear rodlets in mouse models of diabetes. Endocr Pathol 21(4):230-235.

Minsky N, Shema E, Field Y, Schuster M, Segal E, Oren M. 2008. Monoubiquitinated H2B is associated with the transcribed region of highly expressed genes in human cells. Nat Cell Biol 10(4):483-488.

Pal A, Severin F, Lommer B, Shevchenko A, Zerial M. 2006. Huntingtin-HAP40 complex is a novel Rab5 effector that regulates early endosome motility and is up-regulated in Huntington's disease. J Cell Biol 172(4):605-618.

Peters MF, Ross CA. 2001. Isolation of a 40-kDa Huntingtin-associated protein. J Biol Chem 276(5):3188-3194.

Prichett W, Milman P, Gagnon J, Munoz DG, Woulfe J. 2007. Intranuclear rodlets in human pancreatic islet cells. Pancreas 35(3):207-211.

Roncoroni L. 1895. Su un nuovo reperto nel nucleo delle cellule nervose. Arch Psychiatr 16:477.

Sara SJ. 2009. The locus coeruleus and noradrenergic modulation of cognition. Nat Rev Neurosci 10(3):211-223.

Seite R, Leonetti J, Luciani-Vullet J, Vio M. 1977. Cyclic AMP and ultrastructural organization of the nerve cell nucleus: stimulation of nuclear microtubules and microfilaments assembly in sympathetic neurons. Brain Res 124(1):41-51.

Seite R, Mei N, Couineau S. 1971. [Quantitative modification of intranuclear rodlets of sympathetic neurons during electric stimulation]. Brain Res 34(2):277-290.

Spector DL. 1993. Macromolecular domains within the cell nucleus. Annu Rev Cell Biol 9:265-315.

Tong Y, Ha TJ, Liu L, Nishimoto A, Reiner A, Goldowitz D. 2011. Spatial and temporal requirements for huntingtin (Htt) in neuronal migration and survival during brain development. J Neurosci 31(41):14794-14799.

van der Horst A, de Vries-Smits AM, Brenkman AB, van Triest MH, van den Broek N, Colland F, Maurice MM, Burgering BM. 2006. FOXO4 transcriptional activity is regulated by monoubiquitination and USP7/HAUSP. Nat Cell Biol 8(10):1064-1073.

Villagra NT, Bengoechea R, Vaque JP, Llorca J, Berciano MT, Lafarga M. 2008. Nuclear compartmentalization and dynamics of the poly(A)-binding protein nuclear 1 (PABPN1) inclusions in supraoptic neurons under physiological and osmotic stress conditions. Mol Cell Neurosci 37(3):622-633.

Woulfe J, Gray D, Prichett-Pejic W, Munoz DG, Chretien M. 2004. Intranuclear rodlets in the substantia nigra: interactions with marinesco bodies, ubiquitin, and promyelocytic leukemia protein. J Neuropathol Exp Neurol 63(11):1200-1207.

Woulfe J, Munoz D. 2000. Tubulin immunoreactive neuronal intranuclear inclusions in the human brain. Neuropathol Appl Neurobiol 26(2):161-171.

Woulfe JM, Hammond R, Richardson B, Sooriabalan D, Parks W, Rippstein P, Munoz DG. 2002. Reduction of neuronal intranuclear rodlets immunoreactive for tubulin and glucocorticoid receptor in Alzheimer's disease. Brain Pathol 12(3):300-307.

Woulfe JM, Prichett-Pejic W, Rippstein P, Munoz DG. 2007. Promyelocytic leukaemia-immunoreactive neuronal intranuclear rodlets in the human brain. Neuropathol Appl Neurobiol 33(1):56-66.

Zhou W, Zhu P, Wang J, Pascual G, Ohgi KA, Lozach J, Glass CK, Rosenfeld MG. 2008. Histone H2A monoubiquitination represses transcription by inhibiting RNA polymerase II transcriptional elongation. Mol Cell 29(1):69-80.

General discussion.

INRs are intriguing, yet little studied nuclear structures. As discussed in the Introduction, changes in INR frequency are associated with changes in cellular function brought about by a number of physiological and pathological stimuli suggesting a functional role for INRs in the regulation of cellular activity. Some of the more recent observations include up-regulation of INR frequency in a mouse model of Parkinson's disease, the loss of INRs in Alzheimer's disease and in mouse models of human metabolic syndrome. Still, more than a century after INRs were first documented their physiological function, protein composition and mechanism of action remain unknown.

Given this current rudimentary state of understanding of most aspects of INR biology (with the notable exception of its ultrastructure), I set out to establish a basic experimental framework to facilitate a systematic approach to these questions. Experimental models or biological systems in which INR expression can be predictably altered by well-defined experimental manipulations needed to be established. To do this, I started with a biological system that was known to express INRs, the endocrine pancreas, and then looked for conditions in which INR expression would be altered in this system. Investigation of the effects of a broad spectrum metabolic regulator of b-cell structure and function, liver kinase B-1 (Lkb-1), yielded several experimental models of altered β-cell INR expression that are now available for further study.

The LABKO mouse created in the laboratory of Dr. Robert Screaton is an *in vivo* model in which specific adult β-cell knock out of a metabolic master-regulator kinase Lkb-1 resulted in significant depletion of β-cell INRs. The LABKO mouse model of altered β-cell INR expression, therefore, represents a starting point to elucidate more specifically the proximate signalling

pathways regulating INR formation. Lkb-1 has multiple cellular targets that include other kinases such as members of the 5' AMP-activated protein kinase (AMPK) family (Lizcano et al 2004). Together these kinases target multiple substrates controlling a number of downstream effectors. Two of these effectors, Mark2 and mTOR, have been shown to be responsible for the altered β-cell polarity and β-cell hypertrophy respectively described in LABKO mice. Accordingly, Mark2 and mTOR were investigated as potential regulators of INR expression. INR expression was unaffected in Mark2 knockout mice. mTOR, on the other hand, appeared to regulate INR expression independently of the Lkb-1 effect on INRs. mTOR activity is elevated in LABKO β-cells presumably due to alleviation of AMPK mediated inhibition of the mTOR pathway. The resulting β-cell hypertrophy was rescued by a specific mTOR inhibitor, rapamycin. Rescue of INR expression by rapamycin would be expected if mTOR were the downstream effector of the INR depletion phenotype in the Lkb1 knock out. Instead, further reduction of INR expression was observed following inhibition of mTOR activity with rapamycin in LABKO mice. Therefore it was concluded that 1) the mTOR pathway is implicated as an independent regulator of INR expression; and 2) the loss of INRs observed in Lkb-1 knock out β-cells is not mediated through downstream mTOR activation. Thus mTOR and Lkb-1 are independent pathways of INR regulation and should be further investigated independently from one another.

Another important finding was the observed depletion of INRs from the b-cells in two commonly employed models of human metabolic syndrome associated with obesity related diabetes. The ob/ob model is of particular interest because of the remarkable degree of INR depletion. The observed depletion of INRs in two etiologically distinct models of early stages of obesity related diabetes may be indicative of a common regulatory event associated with diabetic β-cell transformation as being responsible for INR downregulation. In this respect the compensatory upregulation of insulin release, islet β-cell hypertrophy and hyperplasia observed

in these models warrant further investigation as potential regulators of INR expression. However, the possibility that INR depletion from β-cells in these two mouse models of diabetes is triggered by distinct mechanisms cannot be excluded. Regardless of the mechanism, these findings suggest a possible involvement of INRs in the pathogenesis of the human metabolic syndrome, thus strengthening the case for further investigation of β-cell INRs and their relationship to the mechanisms involved in β-cell dysfunction.

My studies have expanded the evidence suggesting that INRs are a biochemically heterogeneous family of intranuclear bodies sharing a common structural morphology. I have described a new biochemically distinct subtype of INR, immunoreactive for Hap40, and provided evidence for additional INR subtypes whose defining immunological markers have not as yet been identified but which share ubiquitin immunoreactivity as a common feature. Biochemical heterogeneity of INRs is an important concept with potentially far reaching repercussions for the study of their functional significance. This concept was first brought to light by the observations of SDL.3D10 negative PABPN1 positive INRs in oxytocin producing magnocellular SON neurons (Berciano et al. 2004). Further observation of cell type specific, mutually exclusive expression of SDL- and PABPN1-INRs in parvocellular vs. oxitocinergic magnocellular neurons of the SON suggested that these two types of INRs may in fact perform distinct, cell type-specific functions. The discovery of yet another biochemically distinct subtype of INR with a cell type-specific distribution lends further support to the concept of cell type-specific, biochemically defined functional heterogeneity of the INR family of nuclear bodies.

Taking into consideration the aforementioned biochemical heterogeneity; the evolutionary pervasiveness of INRs; their morphological and ultrastructural similarity; the diverse and at times apparently contradictory aspects of regulation, a unifying model could be constructed. Under this new model, I propose that INRs appeared early in evolution to serve as a reactive surface for

nuclear proteins in a manner analogous to the way the cellular membrane serves to bring enzymes and their substrates together, as exemplified by cell surface receptor-mediated signalling. During cell surface receptor mediated signalling, chemical modification of the membrane receptor molecule triggered by external stimuli leads to recruitment of specific adapter molecules, enzymes and substrates from a three-dimensional space in the cytosol into the two-dimensional context of the membrane inner surface. This effectively increases enzyme and substrate concentrations resulting in an increased rate of enzymatic reaction. By analogy, INR rods and sheets may serve as scaffolds for adaptor-mediated recruitment of nuclear proteins to facilitate an accelerated rate of nuclear function. Expression of cell type specific INR scaffold adaptor molecules would result in expression of cell type specific INR subtypes in accordance with the functional requirements of the given cell type. Thus biochemically distinct INR subtypes will have evolved on the basis of a common protein scaffold to perform distinct and possibly unrelated nuclear functions. In the context of this hypothesis, identification of the common protein(s) forming this universal scaffold becomes the central task in proving its validity.

The study of the INR family of nuclear bodies is currently in its infancy. The results described in this thesis have set the stage for further investigation into the functional significance of SDL-INRs in pancreatic beta-cells and have highlighted the notion of a biochemical and possibly functional diversity of INRs. Further studies aimed at biochemical and functional characterization of individual INR subtypes would provide insight not only into the biology of the INR itself but the biology of the specific cell types harbouring these enigmatic nuclear bodies.

Bibliography.

Andrews, J.M., and Sekhon, S.S. (1969). Varieties of intranuclear filamentous aggregates in cerebral neurons. Bull Los Angeles Neurol Soc *34*, 163-174.

Berciano, M.T., Villagra, N.T., Ojeda, J.L., Navascues, J., Gomes, A., Lafarga, M., and Carmo-Fonseca, M. (2004). Oculopharyngeal muscular dystrophy-like nuclear inclusions are present in normal magnocellular neurosecretory neurons of the hypothalamus. Hum Mol Genet *13*, 829-838.

Boquist, L. (1969). Intranuclear rods in pancreatic islet beta-cells. The Journal of cell biology *43*, 377-381.

Brown, W.J., Kotorii, K., and Riehl, J.L. (1968). Ultrastructural studies in myoclonus epilepsy. (Clinical Unverricht-Lafora's disease). Neurology *18*, 427-438.

Cajal, S.R. (1909). Histologie du systeme nerveux de l'homme et des vertebres. Consejo Superior de Investigaciones Cientificas, Madrid *1*.

Chandler, R.L. (1966). Intranuclear structures in neurones. Nature *209*, 1260-1261.

Chandler, R.L., and Willis, R. (1966). An intranuclear fibrillar lattice in neurons. Journal of cell science *1*, 283-286.

Clattenburg, R.E., Singh, R.P., and Montemurro, D.G. (1972). Intranuclear filamentous inclusions in neurons of the rabbit hypothalamus. Journal of ultrastructure research *39*, 549-555.

Dahl, E. (1970). The fine structure of nuclear inclusions. Journal of anatomy *106*, 255-262.

David, S., and Nathaniel, E.J. (1978). Intranuclear inclusions in the developing neurons of the rat cuneate nuclei. Cell and tissue research *193*, 525-532.

de Estable-Puig, R.F., and Estable-Puig, J.F. (1970). Close association between nuclear rodlets and chromosomal fibers. Canadian journal of zoology *48*, 590-591.

Dixon, J.S. (1970). Nuclear bodies in normal and chromatolytic sympathetic neurons. Anat Rec *168*, 179-185.

Feldman, M.L., and Peters, A. (1972). Intranuclear rods and sheets in rat cochlear nucleus. Journal of neurocytology *1*, 109-127.

Fiori, M.G. (1987). Intranuclear inclusions in Schwann cells of aged fowl ciliary ganglia. Journal of anatomy *154*, 201-214.

Frink, R., Krupp, P.P., and Young, R.A. (1978). Intranuclear rodlets in woodchuck thyroid follicular cells. Cell and tissue research *193*, 561-563.

Gambetti, P., and Gonatas, N.K. (1967). Fibrils and lattice-like intranuclear structures in nuclei of neurons. Rivista di patologia nervosa e mentale *88*, 188-196.

Ghadially, F.N., ed. (1997). Ultrastructural Pathology of the Cell and Matrix, 4th edn (Boston, Butterworth–Heinemann).

Gutekunst, C.A., Li, S.H., Yi, H., Ferrante, R.J., Li, X.J., and Hersch, S.M. (1998). The cellular and subcellular localization of huntingtin-associated protein 1 (HAP1): comparison with huntingtin in rat and human. J Neurosci *18*, 7674-7686.

Holmgren, E. (1899). Weitere Mitteilungen uber den Bau der Nervenzellen. Anat Anz *16*, 388-397.

Islam, M.S., and Loots du, T. (2009). Experimental rodent models of type 2 diabetes: a review. Methods and findings in experimental and clinical pharmacology *31*, 249-261.

Iwanaga, T., Yamada, J., Yamashita, T., and Misu, M. (1981). Intranuclear filamentous inclusions in the gastro-entero-pancreatic (GEP) endocrine cells of birds. Cell and tissue research *217*, 283-288.

Kim, S.U., Masurovsky, E.B., Benitez, H.H., and Murray, M.R. (1970). Histochemical studies of the intranuclear rodlet in neurons of chicken sympathetic and sensory ganglia. Histochemie *24*, 33-40.

Knox, C.A., Yates, R.D., and Chen, I. (1980). Brain aging in normotensive and hypertensive strains of rats. II. Ultrastructural changes in neurons and glia. Acta neuropathologica *52*, 7-15.

Lafarga, M., Berciano, M.T., and Andres, M.A. (1993). Protein-synthesis inhibition induces perichromatin granule accumulation and intranuclear rodlet formation in osmotically stimulated supraoptic neurons. Anat Embryol (Berl) *187*, 363-369.

Lafarga, M., Berciano, M.T., Garcia-Segura, L.M., Andres, M.A., and Carmo-Fonseca, M. (1998). Acute osmotic/stress stimuli induce a transient decrease of transcriptional activity in the neurosecretory neurons of supraoptic nuclei. Journal of neurocytology *27*, 205-217.

Lafarga, M., and Palacios, G. (1977). Intranuclear rodlets in retrochiasmatic area neurons of the hypothalamus of the rat. Experientia *33*, 1368-1369.

Lamba, W., Prichett, W., Munoz, D., Park, D.S., and Woulfe, J.M. (2005). MPTP induces intranuclear rodlet formation in midbrain dopaminergic neurons. Brain research *1066*, 86-91.

Lane, N.J. (1969). Intranuclear fibrillar bodies in actinomycin D-treated oocytes. The Journal of cell biology *40*, 286-291.

Mann, G. (1894). Histological Changes induced in Sympathetic, Motor, and Sensory Nerve Cells by Functional Activity (Preliminary note). J Anat Physiol *29*, 100-108 101.

Masurovsky, E.B., Benitez, H.H., Kim, S.U., and Murray, M.R. (1970). Origin, development, and nature of intranuclear rodlets and associated bodies in chicken sympathetic neurons. The Journal of cell biology *44*, 172-191.

Pinching, A.J., and Powell, T.P. (1971). Ultrastructural features of transneuronal cell degeneration in the olfactory system. Journal of cell science *8*, 253-287.

Popoff, N., and Stewart, S. (1968). The fine structure of nuclear inclusions in the brain of experimental golden hamsters. Journal of ultrastructure research *23*, 347-361.

Prenant, A. (1897). Cristalloides intranuclkaires des cellules nerveuses sympathiques chez les rnammi- fbres. I: 366. 11. Arch Anat Mikrosk Morphol Exp *1*, 366-373.

Raine, C.S., and Field, E.J. (1968). Nuclear structures in nerve cells in multiple sclerosis. Brain research *10*, 266-268.

Roncoroni, L. (1895). Su un nuovo reperto nel nucleo delle cellule nervose. Arch Psychiatr *16*, 477.

Schuster, F.L., and Dunnebacke, T.H. (1977). Ultrastructural observations of experimental Naegleria meningoencephalitis in mice: intranuclear inclusions in amebae and host cells. J Protozool *24*, 489-497.

Seite, R., Escaig, J., and Couineau, S. (1971a). [Nuclear microfilaments and microtubles and the ultrastructural organization of intranuclear rodlets in sympathetic neurons]. Journal of ultrastructure research *37*, 449-478.

Seite, R., Leonetti, J., Luciani-Vullet, J., and Vio, M. (1977). Cyclic AMP and ultrastructural organization of the nerve cell nucleus: stimulation of nuclear microtubules and microfilaments assembly in sympathetic neurons. Brain research *124*, 41-51.

Seite, R., Mei, N., and Couineau, S. (1971b). [Quantitative modification of intranuclear rodlets of sympathetic neurons during electric stimulation]. Brain research *34*, 277-290.

Seite, R., Mei, N., and Vuillet-Luciani, J. (1973). Effect of electrical stimulation on nuclear microfilaments and microtubules of sympathetic neurons submitted to cycloheximide. Brain research *50*, 419-423.

Siegesmund, K.A., Dutta, C.R., and Fox, C.A. (1964). The Ultrastructure of the Intranuclear Rodlet in Certain Nerve Cells. Journal of anatomy *98*, 93-97.

Sung, J.H. (1980). Light, fluorescence, and electron microscopic features of neuronal intranuclear hyaline inclusions associated with multisystem atrophy. Acta neuropathologica *50*, 115-120.

Tobin, D.J., Mandir, N., Fenton, D.A., and Dover, R. (1991). Intranuclear rodlets and associated true intranuclear bodies in normal cultured human dermal papilla cells. J Invest Dermatol *96*, 388-391.

Toper, S., Bannister, C.M., Lincoln, J., Mann, D.M., and Yates, P.O. (1980). Nuclear inclusions in Alzheimer's disease. Neuropathology and applied neurobiology *6*, 245-253.

Tucker, G.S., Hamasaki, D.I., and Wong, C.G. (1986). Intranuclear rodlets in the rabbit retina following treatment with MPTP. Exp Eye Res *42*, 569-583.

Villagra, N.T., Bengoechea, R., Vaque, J.P., Llorca, J., Berciano, M.T., and Lafarga, M. (2008). Nuclear compartmentalization and dynamics of the poly(A)-binding protein nuclear 1 (PABPN1) inclusions in supraoptic neurons under physiological and osmotic stress conditions. Mol Cell Neurosci *37*, 622-633.

Villagra, N.T., Navascues, J., Casafont, I., Val-Bernal, J.F., Lafarga, M., and Berciano, M.T. (2005). The PML-nuclear inclusion of human supraoptic neurons: a new compartment with SUMO-1- and ubiquitin-proteasome-associated domains. Neurobiol Dis.

Volk, B., and Maletz, J. (1985). Nuclear inclusions following chronic ethanol administration. An electron-microscopic investigation of the rat parietal cortex. Acta neuropathologica *67*, 170-173.

Wajchenberg, B.L. (2007). Beta-cell failure in diabetes and preservation by clinical treatment. Endocrine reviews *28*, 187-218.

Wierup, N., Svensson, H., Mulder, H., and Sundler, F. (2002). The ghrelin cell: a novel developmentally regulated islet cell in the human pancreas. Regulatory peptides *107*, 63-69.

Woulfe, J., Gray, D., Prichett-Pejic, W., Munoz, D.G., and Chretien, M. (2004). Intranuclear rodlets in the substantia nigra: interactions with marinesco bodies, ubiquitin, and promyelocytic leukemia protein. J Neuropathol Exp Neurol *63*, 1200-1207.

Woulfe, J., and Munoz, D. (2000). Tubulin immunoreactive neuronal intranuclear inclusions in the human brain. Neuropathology and applied neurobiology *26*, 161-171.

Woulfe, J.M., Hammond, R., Richardson, B., Sooriabalan, D., Parks, W., Rippstein, P., and Munoz, D.G. (2002). Reduction of neuronal intranuclear rodlets immunoreactive for tubulin and glucocorticoid receptor in Alzheimer's disease. Brain Pathol *12*, 300-307.

Woulfe, J.M., Prichett-Pejic, W., Rippstein, P., and Munoz, D.G. (2007). Promyelocytic leukaemia-immunoreactive neuronal intranuclear rodlets in the human brain. Neuropathology and applied neurobiology *33*, 56-66.

Contributions of collaborators.

For the manuscript contained in chapter 2 we collaborated with Accalia Fu and Robert Screaton who originally created and described the LABKO mice. All tissue sections from treated and untreated LABKO mice and relevant controls were obtained from these collaborators. Tissue sections from Mark2 knockout mice were a kind gift from H. Piwnica-Worms.

Appendix.

Panel 1.

Immunohistochemical staining of brain sections from conditional glucocorticoid receptor (GR) knockout mice and controls using Santa Cruz anti-GR antibody GR P-20.

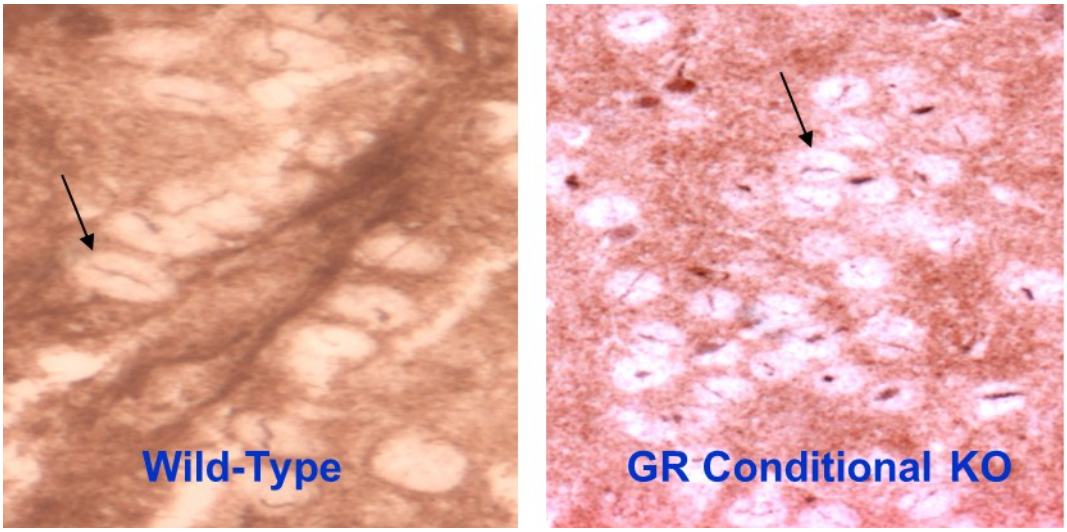

Arrows point to INR-containing neuronal nuclei in both knockout and control brains. Data acquired by John Woulfe.

Panel 2.

Carboxyl-terminal hemagglutinin (HA) tagged Class III β Tubulin (C3T-HA) was transiently overexpressed in Nit1-1 cells. In transfected cells C3T-HA was successfully incorporated into a microtubule-like network, but failed to incorporate into SDL.3D10 immunoreactive INRs.

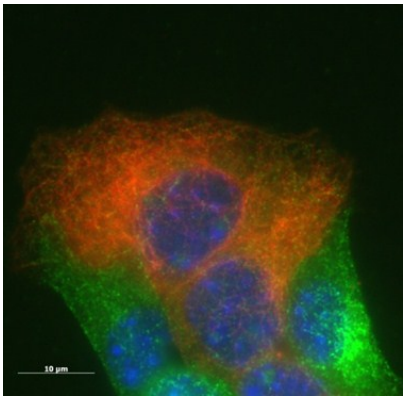

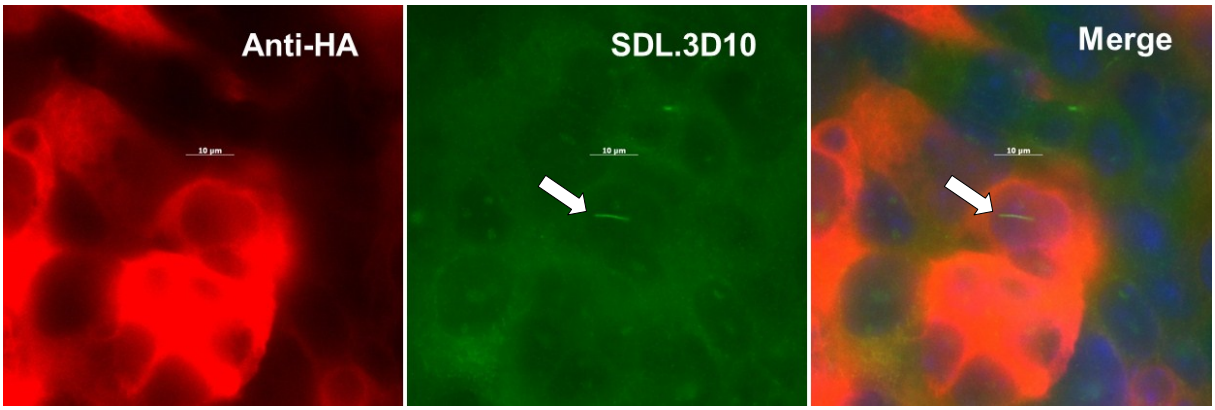

Anti-HA and SDL.3D10 antibodies were detected with AlexaFluor594 (red) and AlexaFluor488 (green) fluorophore labeled secondary antibodies, respectively. Arrows point to an SDL.3D10 positive, HA negative INR. Vector was prepared by Jeff Gagnon. Transfections and immunofluorescence by Pavel Milman.

MILMAN, PAVEL

EDUCATION

2006-present University of Ottawa
Ph.D. Candidate in Biochemistry
Dissertation: "Intranuclear Rodlets: Dynamic Nuclear Bodies in Pancreatic Beta-Cells; and a Novel Variant in Mouse CNS Neurons".

2003-2005 University of Ottawa
M.Sc. Biochemistry
Thesis: "Role and regulation of Adrenomedullin signaling during adipogenic conversion of mouse 3T3-L1 preadipocytes"

1992-1997 University of Toronto Honors
B.Sc. Cell and Molecular Biology
Thesis: "Molecular cloning and characterisation of the cDNA and genomic clones of a gene that isdifferentially expressed in steroid hormone induced differentiation of Achlya ambisexualis".

1989-1990 Pirogov State Medical Institute, Moscow, Russia
Faculty of Medicine and Biology
Completed first year curriculum.

RESEARCH EXPERIENCE

2001-2003 **Graduate Student**
Department of Chemistry, York University, Toronto.

1998-2001 **Research Technician**
Center for Research in Neurodegenerative Diseases, University of Toronto

TECHNICAL EXPERTISE

- Immunofluorescence microscopy
- Mammalian Tissue Culture
- Transient and Stable Transfections
- Metabolic Labelling
- Subcellular fractionation
- Protein extraction from Mammalian Cells and Tissue
- RNA Isolation from Mammalian Cells and Tissue

- Real-Time Quantitative RT-PCR
- Site Directed Mutagenesis
- Primer Extension Analysis
- Cloning
- Expression and Purification of Recombinant Protein
- FPLC Purification of Recombinant Protein
- Prepared and ran samples on SELDI - MS
- Built, exploited, and participated in the design of Capillary Electrophoresis system
- Standard molecular biology and biochemistry techniques (Western Blot, Silver Stain, DNA Digestions, etc.)

LIST OF PUBLICATIONS

1. **Milman, P**., A. Fu, R.A. Screaton, and J.M. Woulfe. 2010. Depletion of intranuclear rodlets in mouse models of diabetes. ***Endocrine pathology*** 21:230-235.
2. Prichett, W., **P. Milman**, J. Gagnon, D.G. Munoz, and J. Woulfe. 2007. Intranuclear rodlets in human pancreatic islet cells. ***Pancreas*** 35:207-211.
3. Chen, F., G. Yu, S. Arawaka, M. Nishimura, T. Kawarai, H. Yu, A. Tandon, A. Supala, Y.Q. Song, E. Rogaeva, **P. Milman**, C. Sato, C. Yu, C. Janus, J. Lee, L. Song, L. Zhang, P.E. Fraser, and P.H. St George-Hyslop. 2001. Nicastrin binds to membrane-tethered Notch. ***Nature cell biology*** 3:751-754.
4. Zhang, D.M., D. Levitan, G. Yu, M. Nishimura, F. Chen, A. Tandon, T. Kawarai, S. Arawaka, A. Supala, Y.Q. Song, E. Rogaeva, Y. Liang, E. Holmes, **P. Milman**, C. Sato, L. Zhang, and P. St George-Hyslop. 2000. Mutation of the conserved N-terminal cysteine (Cys92) of human presenilin 1 causes increased A beta42 secretion in mammalian cells but impaired Notch/lin-12 signalling in C. elegans. ***Neuroreport*** 11:3227-3230.
5. Yu, G., M. Nishimura, S. Arawaka, D. Levitan, L. Zhang, A. Tandon, Y.Q. Song, E. Rogaeva, F. Chen, T. Kawarai, A. Supala, L. Levesque, H. Yu, D.S. Yang, E. Holmes, **P. Milman**, Y. Liang, D.M. Zhang, D.H. Xu, C. Sato, E. Rogaev, M. Smith, C. Janus, Y. Zhang, R. Aebersold, L.S. Farrer, S. Sorbi, A. Bruni, P. Fraser, and P. St George-Hyslop. 2000. Nicastrin modulates presenilin-mediated notch/glp-1 signal transduction and betaAPP processing. ***Nature*** 407:48-54.
6. Yu, G., F. Chen, M. Nishimura, H. Steiner, A. Tandon, T. Kawarai, S. Arawaka, A. Supala, Y.Q. Song, E. Rogaeva, E. Holmes, D.M. Zhang, **P. Milman**, P.E. Fraser, C. Haass, and P.S. George-Hyslop. 2000. Mutation of conserved aspartates affects maturation of both aspartate mutant and endogenous presenilin 1 and presenilin 2 complexes. ***The Journal of biological chemistry*** 275:27348-27353.
7. Yu, G., F. Chen, M. Nishimura, H. Steiner, A. Tandon, T. Kawarai, S. Arawaka, A. Supala, Y.Q. Song, E. Rogaeva, E. Holmes, D.M. Zhang, P. **Milman, P.** Fraser, C. Haass, and P. St

George-Hyslop. 2000. Mutation of conserved aspartates affect maturation of presenilin 1 and presenilin 2 complexes. ***Acta neurologica Scandinavica*** 176:6-11.

8. Nishimura, M., G. Yu, G. Levesque, D.M. Zhang, L. Ruel, F. Chen, **P. Milman**, E. Holmes, Y. Liang, T. Kawarai, E. Jo, A. Supala, E. Rogaeva, D.M. Xu, C. Janus, L. Levesque, Q. Bi, M. Duthie, R. Rozmahel, K. Mattila, L. Lannfelt, D. Westaway, H.T. Mount, J. Woodgett, P. St George-Hyslop, and et al. 1999. Presenilin mutations associated with Alzheimer disease cause defective intracellular trafficking of beta-catenin, a component of the presenilin protein complex. ***Nature medicine*** 5:164-169.

REFERENCES AVAILABLE UPON REQUEST.